

# Implementation and verification of an aeroacoustic noise prediction model for wind turbines

**Fuglsang, Peter; Aagaard Madsen , Helge**

*Publication date:*
1996

*Document Version*
Publisher's PDF, also known as Version of record

Risø-R-867(EN)

RISØ

# Implementation and Verification of an Aeroacoustic Noise Prediction Model for Wind Turbines

Peter Fuglsang and Helge Aagaard Madsen

The Test Station for Wind Turbines

Risø National Laboratory, Roskilde, Denmark
March 1996

# Implementation and Verification of an Aeroacoustic Noise Prediction Model for Wind Turbines

Risø-R-867(EN)

Peter Fuglsang and Helge Aagaard Madsen

Risø National Laboratory, Roskilde, Denmark
March 1996

**Abstract**
The present report concerns a semi-empirical noise prediction model for the aerodynamic noise from wind turbine rotors. It covers both turbulent inflow noise and airfoil self noise. The noise prediction model cooperates with aerodynamic calculations and a design tool based on numerical optimization.

The spectra for different noise sources are determined and the total noise is compared to measurements. Fair agreement is obtained for the sound power level, with deviations within 1.5 dB(A) on the absolute value. The shape of the predicted spectrum fits well to measurements. A sensitivity study on different design parameters is performed. Measurements agree well with predictions for variations of the wind speed, tip pitch angle and tip speed. This is encouraging, since a reliable relative comparison between different rotors seems possible.

By use of a numerical optimization tool for wind turbines, several optimization studies are carried out, with the starting point at an existing 300 kW rotor. Optimizing for minimum noise is possible and this lowers the sound power level by 3 dB(A), a substantial reduction. The resulting rotor has however increased cost and extreme loads. Therefore cost should also be estimated for the noise emission. It is possible to control the resulting sound power level by optimizing for maximum production or minimum cost with constraints on the noise. This allows for inclusion of noise limits from customers or codes of practice directly in the design process. An optimization without noise concerns emphasizes the importance of this, since this increases the noise by 3 dB(A), without a significant improvement in the annual production.

The prediction model is useful for parameter investigations and design studies for a new generation of less noisy wind turbines having low cost. However, the degree of detail for the boundary layer parameters should be increased by application of an airfoil prediction code. Finally, verification should be extended with measurements from rotors with different airfoils.

The EFP program of the Danish Ministry of Energy supported the present work under the contracts:

ENS-1364/93-0006 "Aerodynamisk Støj"
ENS-1364/93-0001 "Rotor Aerodynamik"

ISBN 87-550-2149-2
ISSN 0106- 2840

Grafisk Service, Risø, 1996

# Contents

# 1 Introduction

In the planning of the erection of wind turbines near residential areas, the radiation of noise is an important issue. Although noise radiation by a wind turbine is not large by ordinary standards, it can still be of significance compared to the low background levels that exist in much of the countryside. The radiation of noise is a sales parameter and much effort is going into the design of a new generation of highly efficient, less noisy wind turbines. Thus, there is a need for accurate prediction of the radiated noise from wind turbines placed both individually and in wind farms.

The radiation of noise can be divided into two different principal sources: Mechanical noise and aerodynamic noise. Mechanical noise often radiates from the gearbox. The radiation is well understood and knowledge is incorporated into the design process. However, until recently, understanding of aerodynamic noise has been limited. Empirical prediction methods have consisted of simple algebraic formulas based on tip speed, rotor diameter and rotor power etc.

At the time being, there is no fully established method for the prediction of wind turbine noise. A physical and mathematical basis for noise radiation is available, based on the Navier-Stokes equations. At The Test Station for Wind Turbines, a theory is being developed, where Navier-Stokes equations are solved together with acoustic equations for the noise radiation. This is based on the work of Hardin, [1]. Results are still in an early stage, and the method is not yet fully developed.

However, several empirical models for aerodynamic noise prediction are available. These are mainly developed for application on helicopter rotors and aircraft wings, but they are also valid for wind turbines, even though caution must be taken for the difference in operation conditions. The models have only included the major parameters of the rotor, since a model including the local conditions of the blade was not yet established. In 1989, Brooks, Pope and Marcolini [2] published a complex empirical noise prediction model for airfoil self noise based on Amiet [3] and Ffowcs Williams and Hall [4] among others. Airfoil self noise is due to the interaction between an airfoil blade and the turbulence produced in its own boundary layer and near wake. Experimental values for the boundary layer parameters of the NACA 0012 airfoil was in [2] used for calibration and scaling of the model to relate the overall flow conditions with the radiated noise.

Lowson, 1993 [5] and 1994 [6] has further developed an empirical noise prediction method. Instead of experimental results for airfoil boundary layer parameters, an airfoil calculation code is used for prediction. In this way, the model has become more applicable to blades having up-to-date airfoils rather than the rather aged NACA 0012. Lowson has furthermore extended several elements of the noise prediction and included the noise from turbulent inflow, based on Amiet [3]. Turbulent inflow noise is noise from the turbulence in the oncoming flow at all frequencies being transferred to noise by the rotor blades.

The subject of the present work is to develop a calculation complex, that offers an estimate of the total aerodynamic noise from a wind turbine rotor. It is chosen to apply the Brooks, Pope and Marcolini [2] empirical prediction model for airfoil self noise to wind turbine usage. Their standard model is used as a basis and insufficient partial models should be improved in later work. Further developments have taken place since 1989, where the Brooks, Pope and Marcolini model was published.

Furthermore, noise from the turbulent inflow is included following Lowson [5].

One important intention of the present work is the use of advanced optimization tools in the design process, based on numerical optimization algorithms [7]. Here it would be beneficial to include the noise emission as the optimization objective for minimization, or to add constraints to the noise emission. A correct value of the radiated noise might not be achievable. The ability to perform a reliable relative comparison is however valuable. Noise emission for different blade designs can then be compared in parameter variations and in optimization studies. As a first step, it is assumed that the Brooks, Pope and Marcolini approach [2] is sufficient. It is however realized, that an accurate estimate of the noise probably requires a further refinement of today's noise prediction models.

The report contains of the following chapters:

Chapter 2: A brief description of the different elements in the noise prediction model with focus on the physics of the noise mechanisms and the aerodynamic input parameters for the noise prediction.

Chapter 3: Application of the noise prediction model with an aerodynamic calculation code and the implementation of the noise directivity.

Chapter 4: Verification of the noise prediction model together with sensitivity analysis on the noise emission calculation to the aerodynamic input and to the rotor operation conditions.

Chapter 5: Design optimization of a rotor where considerations are taken to noise emission, which is either minimized or constrained.

Chapter 6: Concluding remarks.

# 2 Aerodynamic noise prediction model

This chapter contains a brief description of the aerodynamic noise prediction model. Detailed information can be found in the given references. The different noise sources are explained and related to the rotor aerodynamics. The noise sources divide into airfoil self noise and turbulent inflow noise [9]. Prediction of airfoil self noise is based on the work by Brooks, Pope and Marcolini [2], whereas prediction of noise from turbulent inflow is based on Lowson [5]. Finally, the directivity for trailing edge noise is explained.

The model is limited only to the rotor, since this is the object of interest. Therefore, noise contributions from tower shadow, tower and nacelle are not included. It can be assumed that the noise radiation process for any blade section on the wind turbine becomes identical to that for an equivalent airfoil section [5]. Thus summation of the noise from a number of blade element airfoil sections leads to the total sound radiated from a rotor.

## 2.1 Airfoil self noise sources

Airfoil self noise is due to the interaction between an airfoil and a smooth undisturbed flow. The interaction produces turbulence in the airfoil boundary layer and near wake. The airfoil self noise is mainly broadband. The total noise divides into a number of different sources. At high Reynolds numbers, turbulent boundary layers develop over most of the airfoil suction and pressure sides. This produces noise as the turbulence passes the trailing edge. At low Reynolds numbers, mainly laminar boundary layers develop. Their instabilities result in vortex shedding and associated noise from the trailing edge. At modest to high angles of attack, separation from the airfoil suction side can occur. The shedding of vortices produces additional noise from the trailing edge. Another noise source is vortex shedding occurring in the small separated flow region downstream of a blunt trailing edge. Finally, the formation of the tip vortex at the end of a finite lifting span produces noise by interaction with the trailing edge near the tip.

Brooks, Pope and Marcolini based their semi-empirical prediction model for airfoil self noise on a number of experiments, conducted in a wind tunnel environment. The NACA 0012 airfoil was investigated for different aspect ratios and Reynolds numbers, with both tripped and untripped flow. The radiated noise was measured by several microphones. In addition, the airfoil boundary layer velocity profile was measured by use of hot-wire equipment, and boundary layer parameters were determined.

Scaling laws, based on the fundamentals of aeroacoustics have been establish for the different noise sources. Through the experiment, the sound pressure levels from the different noise sources have were with scaling parameters. The scaling law prediction equations were then fitted to the noise spectra and either the boundary layer thickness, $\delta$, or the boundary layer displacement thickness, $\delta^*$ with empirical constants/ functions. These scaling parameters were then fitted as a function of angle of attack and Reynolds number. In this way, the sound pressure level is estimated by simple knowledge of the airfoil gross flow.

A considerable part of the experimental data relates to low Reynolds numbers and low incidence. Furthermore, the majority of the data used, refer to boundary layer cases where the flow was tripped. The calibration with the scaling parameters should therefore be looked upon with caution, especially at high incidence and

high Reynolds number. It is likely that the empirical factors used and hence, the boundary layer characteristics, depend on the airfoil shape and use of the model should therefore be restricted to airfoils similar to the NACA 0012.

**Turbulent boundary layer trailing edge noise (TBL-TE)**

Noise radiation from the turbulence in the boundary layer flow origins from the interaction of the turbulence, on both the pressure and the suction side, with the trailing edge when the blade-attached turbulent boundary layer convects into the wake. This is illustrated in Figure 2-1.

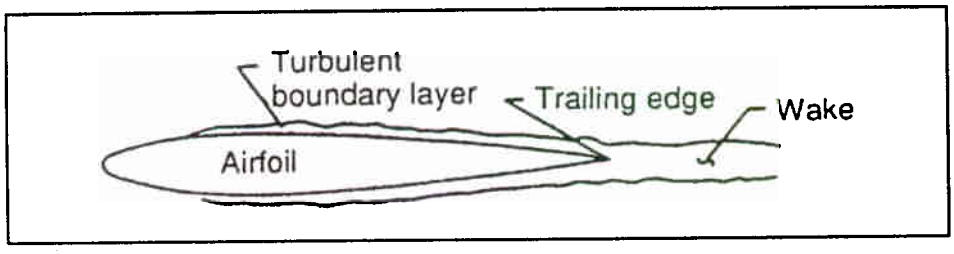


*Figure 2-1* *Turbulent boundary layer trailing edge noise from both the pressure and the suction side of the airfoil section [2].*

The frequency spectrum is broadband, with peak level at intermediate frequencies. The contribution to the overall sound pressure level is not considered important at low Reynolds numbers, but significant at high Reynolds numbers.

The edge-scatter formulation by Ffowcs Williams and Hall [4] is used to establish a relation between the overall sound pressure level on velocity to the fifth power. This theory is valid at low Mach numbers. The sound pressure level ($L_p$) can be found, using a normalization form, here written for the pressure side of the airfoil, at zero angle of attack:

$$(L_P)_P = 10\log\left(\frac{\delta_p^* M^5 L\overline{D}_h}{r_e^2}\right) + A\left(\frac{St_p}{St_1}\right) + (K_1 - 3) + \Delta K_1 \qquad (2\text{-}1)$$

Where $\delta_p^* = \delta_p^*(\alpha, Re_c)$ is the boundary layer displacement thickness, $\alpha$ is the angle of attack, $Re_c$ is the Reynolds number based on chord, $M = U/c_o$ is the Mach number, $U$ is the free stream velocity, $c_o$ is the speed of sound, $L$ is the length of the span, $D_h$ is the directivity, $r_e$ is the retarded observer distance, $A()$ is the universal frequency spectrum shape, $St_p = (f\delta_p^*)/U$ is the Strouhal number based on the displacement thickness, $f$ is the frequency, $St_1 = 0.02M^{-0.6}$, $K_1 = K_1(Re_c)$ and $\Delta K_1 = \Delta K_1(\alpha, Re_{\delta_p^*})$ are empirical functions.

An equivalent expression is found for the suction side and for angles of attack not equal to zero.

The total sound pressure level from turbulent trailing edge noise is then found from:

$$(L_P)_{TBL-TE} = 10\log\left(10^{(L_P)_\alpha/10} + 10^{(L_P)_s/10} + 10^{(L_P)_p/10}\right) \quad (2\text{-}2)$$

Where $(L_P)_s$ is the sound pressure level from the suction side and $(L_P)_\alpha$ is the sound pressure level from an angle of attack not equal to zero.

The rotor aerodynamic parameters for determination of the sound pressure level from turbulent boundary layer trailing edge noise for a blade segment are:

- Angle of attack
- Chord
- Span
- Free stream velocity
- Directivity (section 2.3)
- Retarded observer distance (section 2.3)

**Separated flow noise**

An airfoil at modest to high angles of attack might stall and have a zone of separated flow on the suction side. This zone contains recirculating low momentum fluid, and the flow picture is highly unsteady. Noise from this separation zone is due to the shedding of vortices from the airfoil trailing edge into the wake, as shown in Figure 2-2. Turbulence scales at the trailing edge increase as the angle of attack increases. At deep stall conditions, unsteady flow exists above the entire suction side. The noise is then radiated from the chord as a whole.

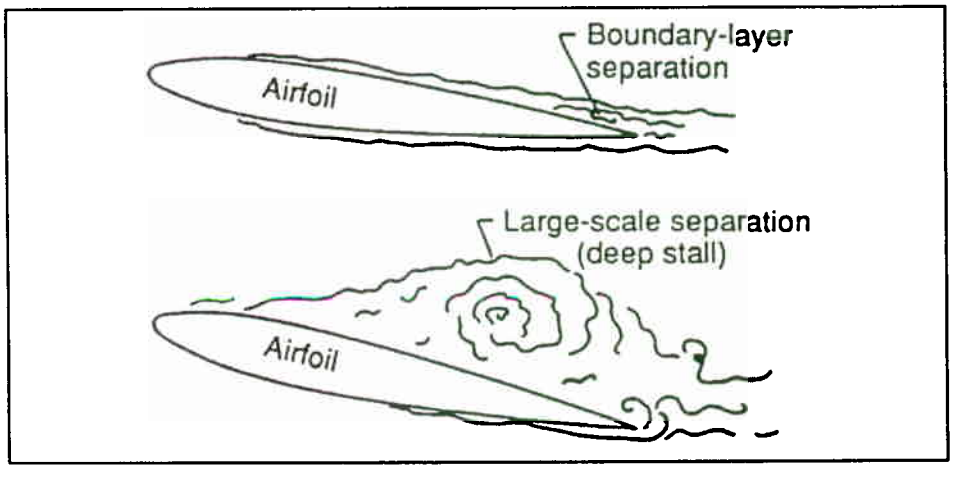


*Figure 2-2* *Separated flow noise from an airfoil at moderate to high angles of attack [2].*

The radiated noise is broadband and only significant at high angles of attack. The peak frequency is typically intermediate to low.

A predictive method was not yet developed. Instead, the formulation for $(L_P)_\alpha$ on the same form as eq. (2-1) for an attached boundary layer is used. For angles of

attack larger than 12.5°, an independent scaling of $(L_P)_\alpha$ for a separated boundary layer was carried out [2].

The rotor aerodynamic parameters for the noise prediction are the same as in the previous section.

**Laminar boundary layer vortex shedding noise (LBL-VS)**

When a laminar boundary layer exists over at least one side of an airfoil, vortex shedding noise can occur, Figure 2-3. This vortex shedding is coupled to a local aeroacoustic instability within the boundary layer driven by the trailing edge in acoustically exited aerodynamic feedback loops. The acoustic wave travels upstream from the trailing edge and couples to the Tollmien-Schlicting instabilities in the upstream laminar boundary layer. These waves grow exponentially down stream and finally they regenerate an upstream acoustic wave as they reach the trailing edge. The instability wave normally appears on the pressure side of the airfoil. The turbulent boundary layer on the suction surface can then be regarded as a broadband starting mechanism [5].

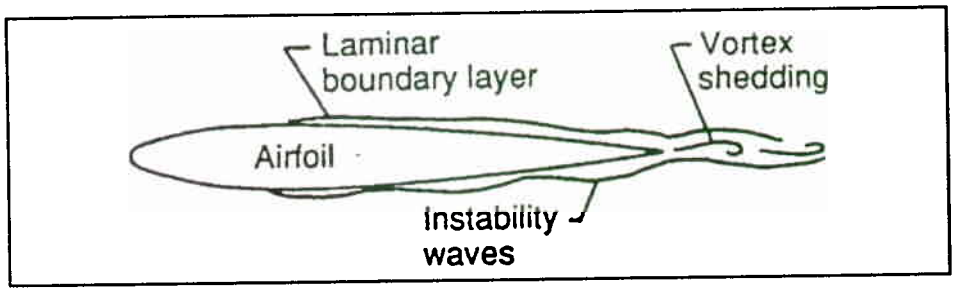


*Figure 2-3* *Laminar boundary layer vortex shedding noise from an airfoil with laminar flow on at least one side [2].*

The resulting noise spectrum is composed of quasi-tones related to the shedding rates at the trailing edge. These tones are often of high frequencies, typically between 1000 - 5000 Hz depending on Reynolds number and angle of attack. Hence, they can be of importance to the overall sound pressure level.

A scaling method is was yet developed for laminar vortex shedding noise explicitly. It was found that the frequency dependence scales on a Strouhal number basis with the boundary layer thickness at the trailing edge as length scale [2].

The sound pressure level is found from:

$$(L_P)_{LBL-VS} = 10\log\left(\frac{\delta_p M^5 L\overline{D}_h}{r_e^2}\right) + G_1\left(\frac{St'}{St'_{peak}}\right) + G_2\left(\frac{\mathrm{Re}_c}{(\mathrm{Re}_c)_0}\right) + G_3(\alpha) \qquad (2\text{-}3)$$

Where $\delta_p$ is the pressure side boundary layer thickness, $G_1()$, $G_2()$ and $G_3()$ are empirical functions, $St' = St'(Re_c)$ is the Strouhal Number, $St_{peak}' = St_{peak}'(\alpha)$ is the peak Strouhal number, $(Re_c)_0 = (Re_c)_0(\alpha)$ is the reference Reynolds number.

The necessary rotor aerodynamic parameters for determination of the sound pressure level from laminar boundary layer vortex shedding noise for a blade segment are:

- Angle of attack
- Chord
- Span
- Free stream velocity
- Directivity (section 2.3)
- Retarded observer distance (section 2.3)

**Tip vortex formation noise**

The flow over the blade tip consists of a vortex shed from the trailing edge at the end of the finite lifting span as shown in Figure 2-4. Interaction between the tip vortex and the trailing edge causes the tip noise. The tip noise source is identified with the turbulence in the local separated flow associated with the strength of the tip vortex at the trailing edge.

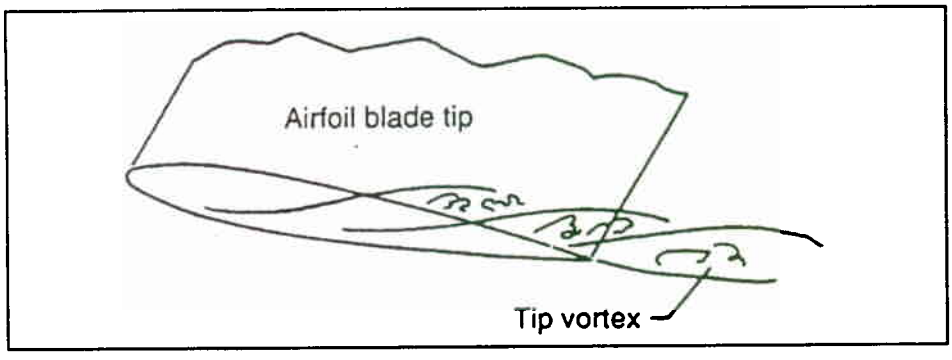


*Figure 2-4 Tip vortex noise from the ending of a finite lifting span [2].*

The noise spectrum is broadband, dominated by higher frequencies, typically at around 4000 Hz, depending on tip speed. The sound pressure level from tip noise is not significant compared to the turbulent trailing edge noise. However, the higher frequencies are of importance to environmental issues rather than low frequencies.

The prediction method used was developed by Brooks and Marcolini [8]. The noise is associated with the spanwise extent of the separated flow region at the tip trailing edge.

The sound pressure level is found from:

$$(L_P)_{TIP} = 10\log\left(\frac{M^2 M_{max}{}^5 l^2 \overline{D}_h}{r_e{}^2}\right) - 30.5(\log St'' + 0.3)^2 + 126 \qquad (2\text{-}4)$$

Where $M_{max} = M_{max}(\alpha_{tip})$ is the maximum Mach number, $l = l(\alpha_{tip})$ is the spanwise extent of the separation zone, $St'' = f\,l/U_{max}$ is the Strouhal number, $U_{max}$ is the maximum velocity in the vicinity of the tip vortex.

$l(\alpha_{tip})$ furthermore depends on whether the tip edge is rounded or sharp.

The rotor aerodynamic parameters for determination of the tip noise are:

- Angle of attack for the tip section
- Tip chord
- Velocity of the oncoming flow at the tip
- Directivity (section 2.3)
- Retarded observed distance (section 2.3)
- Tip shape

The angle of attack is the geometric angle of attack for an untwisted lifting span corresponding to the experiments. This is difficult to determine for a twisted blade, since the angle of attack variation is large from root to tip. Therefore an equivalent angle of attack should be chosen.

**Trailing edge bluntness vortex shedding noise (TEB-VS)**

Vortices are shed from a blunt trailing edge. This produces noise as the coherent vortex shedding causes a fluctuating surface pressure differential across the trailing edge. This can cause tonal radiation of discreet frequencies at the trailing edge, even for turbulent boundary layers, as shown in Figure 2-5. The effect of the trailing edge geometry is particularly significant, and a number of investigations have been performed. However, a satisfactory prediction method is not yet developed [5].

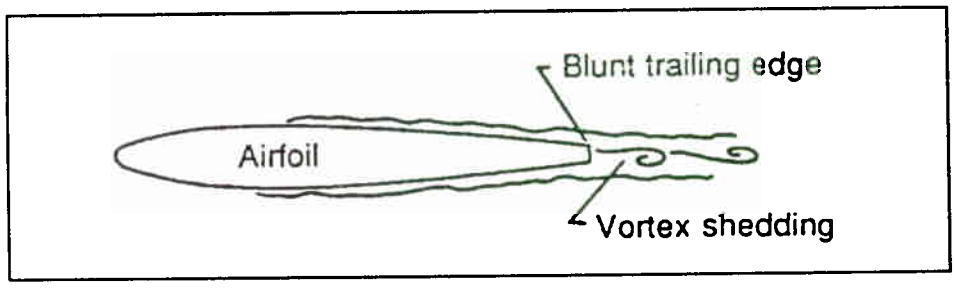


*Figure 2-5* *Trailing edge bluntness vortex shedding noise from a blunt trailing edge [2].*

The noise spectrum is a combination of a broadband area and a peak frequency corresponding to a tone. This frequency is intermediate to high [3].

An expression for the sound pressure level was found by [2]. Scaling parameters are the trailing edge thickness and the boundary layer displacement thickness:

$$(L_P)_{TEB-VS} = 10\log\left(\frac{hM^{5.5}L\bar{D}_h}{r_e^{\,2}}\right) + G_4\left(\frac{h}{\delta^*_{avg}}, \Psi\right) + G_5\left(\frac{h}{\delta^*_{avg}}, \Psi, \frac{St'''}{St'''_{peak}}\right) \qquad (2\text{-}5)$$

Where $h$ is the trailing edge gab, $\delta^*_{avg}$ is the average displacement thickness for the suction and pressure side, $\Psi$ is the solid angle between the sloping surfaces upstream of the trailing edge, $St''' = f\,h/U$ is the Strouhal number.

The aerodynamic input is:

- Trailing edge thickness
- Angle of trailing edge
- Angle of attack
- Chord
- Length of span
- Directivity (section 2.3)
- Retarded observer distance (section 2.3)

## 2.2 Turbulent inflow noise

Turbulence is a part of the natural wind environment. The passage of turbulence causes unsteady pressures on the wind turbine blades, leading to radiation of noise. The rotor transfers the energy in the turbulence at all frequencies into noise. This fluctuating force mechanism is a well-known source for rotor noise. It is significant to the overall wind turbine noise [5]. The wind has a wide range of natural wavelengths, ranging from millimeters to kilometers, whereas the principal energy in the natural turbulence is contained in the large eddies of around 100 m [6]. However, the scale of interest for noise emission is four orders of magnitudes less and focus should be directed towards frequencies within this area.

The resulting noise is broadband, despite low frequency harmonics of the rotational speed from blade to blade interaction. At high power levels or high wind speeds, turbulence ingestion is normally the most important source of noise from the wind turbine [5].

The mechanism for noise radiation from turbulent inflow for an entire rotor is complex. Effects from the flow expansion through the turbine and the blade to blade correlation on the response should be accounted for. A theory is not yet developed, and the present model, used by Lowson [5], based on Amiet [3], concerns an airfoil section. Only first order effects in the turbulence interaction process are included. The sound pressure level from each section is then accumulated to the total sound pressure level.

At high frequencies, the sound pressure level can be found from [3]:

$$(L_p)^H{}_{INFLOW} = 10\log\left(\rho_0{}^2 c_0{}^2 l \, d/r_e{}^2 \, M^3 u^2 l^2 K^3 \left(1+K^2\right)^{-7/3}\right) + 58.4 \qquad (2\text{-}6)$$

Where $\rho_0$ is the air density, $l$ is the overall scale of the turbulence, $u$ is the mean wind speed, $I$ is the turbulence intensity, $K=\pi fc/U$ is the wave number.

At low frequencies, the following expression is used [3]:

$$(L_P)^L{}_{INFLOW} = (L_P)^H{}_{INFLOW} + 10\log LFC$$

$$LFC = 10S^2MK^2\beta^{-2}$$

$$S^2 = \left[\frac{2\pi K}{\beta^2} + \left(1 + 2.4\frac{K}{\beta^2}\right)^{-1}\right]^{-1}$$

(2-7)

Where $LFC$ is a low frequency correction factor, $S$ is the compressible Sears function, $\beta^2 = 1\text{-}M^2$.

A smooth transition between low and high frequency is obtained by:

$$(L_P)_{INFLOW} = (L_P)^H{}_{NFLOW} + 10\log\left(\frac{LFC}{1+LFC}\right)$$

(2-8)

The aerodynamic input for determination of the noise from turbulent inflow is:

- Chord
- Span
- Free stream velocity
- Turbulence length scale
- Turbulence intensity
- Directivity (section 2.3)
- Retarded observer distance (section 2.3)

## 2.3 Noise directivity

A common parameter for the different sound sources is the directivity and the retarded observer distance. These will be defined in the following.

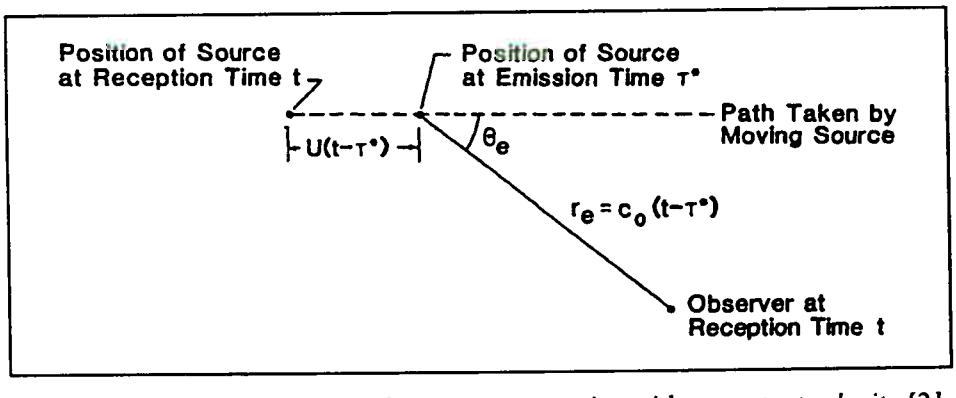


*Figure 2-6* *Noise emission from a source moving with a constant velocity [2].*

In Figure 2-6, a source at the trailing edge of an airfoil is emitting noise. The airfoil is placed in fluid extending to infinity. Thus, there is no wind tunnel shear layer present. The source is emitting noise at time, $\tau^*$ at point A. The ray that reaches the

observer follows the angle, $\Theta_e$ and travels the distance, $r_e$. If the airfoil is moving with the velocity U, when the observer receives the noise, the source has moved $U(t-\tau^*)$ to point B.

Brooks, Pope and Marcolini [2] treat this using a retarded coordinate system, equal to the emission time coordinates, where the positions of the source and the observer are corrected. This takes into account the Doppler related frequency shifts due to the relative motion between the source and the observer.

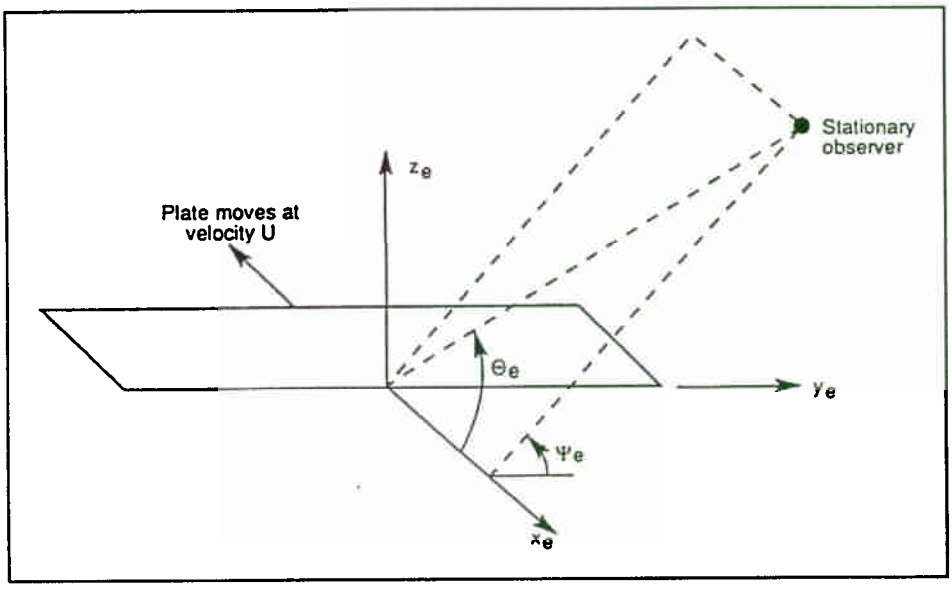


*Figure 2-7* *Flat plate in rectilinear motion shown in a 3-dimensional retarded coordinate system.*

In Figure 2-7, a 3-dimensional retarded coordinate system is defined. The origin is located at the trailing edge of a thin flat plate, representing an airfoil. The plate is in rectilinear motion of velocity U in direction of the negative $x_e$-axis. The observer is stationary.

For high frequencies, the directivity can be shown to be [2]:

$$\overline{D}_H(\Theta_e,\Phi_e) \approx \frac{2\sin^2(\tfrac{1}{2}\Theta_e)\sin^2\Psi_e}{(1+M\cos\Theta_e)\left[1+(M-M_c)\cos\Theta_e\right]^2} \qquad (2\text{-}9)$$

Where $M$ is the Mach number for the plate motion, $M_c$ is the Mach number for the flow past the plate trailing edge, $\Theta_e$ and $\Psi_e$ are the directivity angles shown in Figure 2-7.

The $x_e$-axis should be fixed along the airfoil chord line, rather than with the direction of motion. Application of eq. (2-9) with an angle of attack should result in only little additional error compared to the error already introduced in the relation.

The directivity for low frequencies can be found from [2]:

$$\overline{D}_L(\Theta_e,\Phi_e) \approx \frac{\sin^2\Theta_e \sin^2\Psi_e}{(1+M\cos\Theta_e)^4}$$

*(2-10)*

Eq. (2-9) was derived with the plate assumed to be semi-infinite. $D_H$ becomes inaccurate at shallow upstream angles, when $\Theta_e \rightarrow 180^\circ$. It is used for all airfoil self noise sources except for separation noise, where the angle of attack can be increased significantly. Here, eq. (2-10) is used [2].

# 3 Application with aerodynamic calculation code

This chapter explains the application of the different noise sub models with the aerodynamic calculation of the flow through the rotor. Furthermore, the directivity is explained, with the transformation from the local airfoil trailing edge coordinates to the observer position.

## 3.1 Aerodynamic calculation

The aerodynamic noise prediction model is interfaced with the aerodynamic calculation code, "ROTOR", for optimum rotor design, developed at Risø [7]. This calculation complex consists of a number of sub models for extreme and fatigue loads calculation, estimation of cost, structural and aerodynamic calculations. In addition, it contains a numerical optimization algorithm for design purposes. The aerodynamic calculation model is based on standard strip theory and momentum theory, with empirical corrections for tip loss and high thrust. It is found sufficiently accurate and it provides the input necessary for the noise calculation model.

The total noise from a blade is calculated by dividing the blade into blade elements. The flow across each blade element is found from strip theory and the sound pressure level is calculated by summing the different sources:

$$(L_P)^i_{TOTAL} = 10\log\left(10^{(L_P)_{TBL\text{-}TE}/10} + 10^{(L_P)_{LBL\text{-}VS}/10} + 10^{(L_P)_{TIP}/10} + 10^{(L_P)_{TEB\text{-}VS}/10} + 10^{(L_P)_{INFLOW}/10}\right) \quad (3\text{-}1)$$

The tip noise contribution is only calculated for the last blade segment.

Often, some of the sources might be omitted, e.g. when the flow is tripped, the laminar boundary layer vortex shedding noise is neglected.

The total sound pressure level for a blade is then found:

$$(L_P)_{TOTAL} = 10\log\sum_{i=1}^{n} 10^{(L_P)^i_{TOTAL}/10} \quad (3\text{-}2)$$

Where n is the number of blade elements.

In total, the necessary aerodynamic parameters for each section are:

- The angle of attack for the oncoming flow
- The free stream velocity for the oncoming flow
- The section chord
- The section spanwise length
- The retarded distance to the observer
- The directivity angles
- The trailing edge bluntness

In the present work, the trailing edge bluntness is given as a percentage of the chord.

In addition the following overall parameters are needed:

- A representative geometric angle of attack for the tip noise calculation.
- The shape of the tip edge, rounded/ sharp
- The leading edge flow condition, tripped/ untripped
- The average angle of the trailing edge
- Viscosity of air
- Density of air
- The length scale of the oncoming turbulence
- The intensity of the oncoming turbulence

To find the total noise from the entire rotor, the noise from one blade is calculated at a number of different azimuth stations and an average sound pressure level is found by taking into account the actual number of blades.

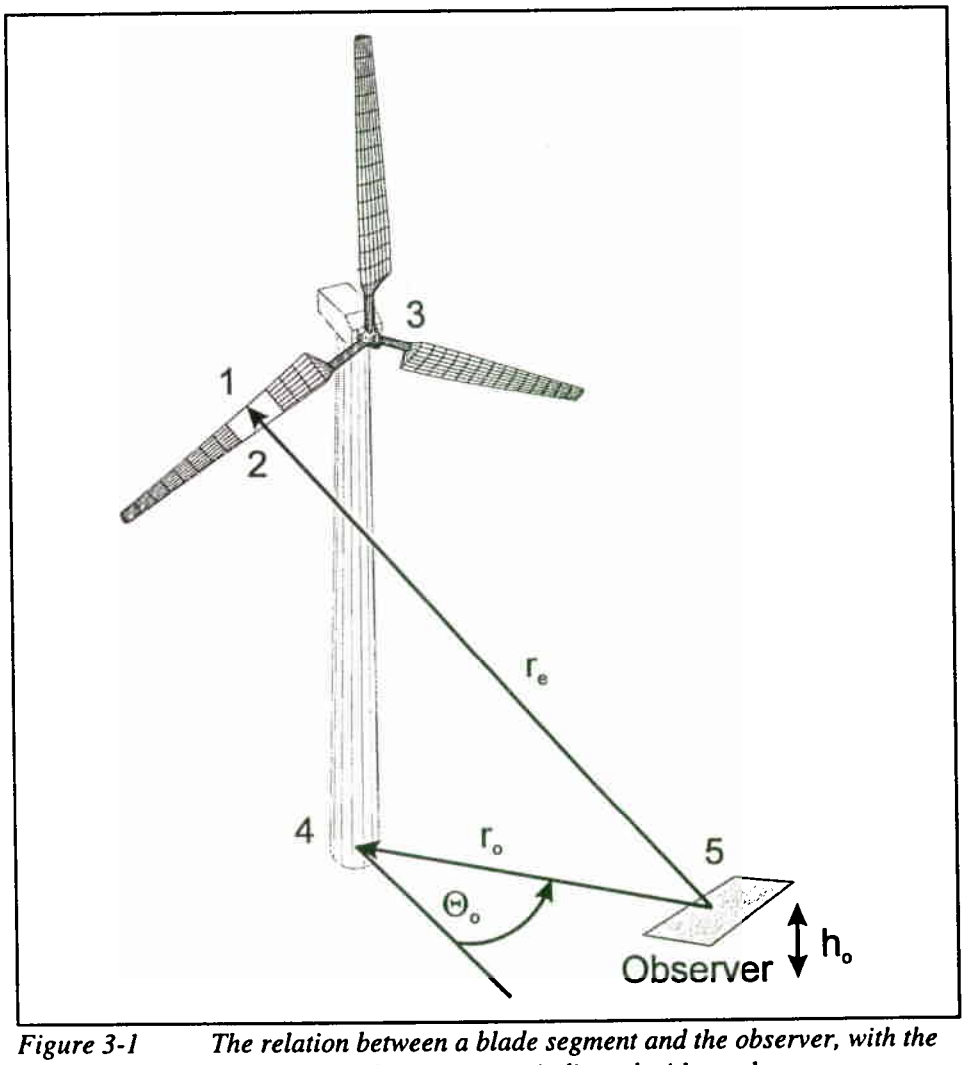


*Figure 3-1* *The relation between a blade segment and the observer, with the different coordinate systems indicated with numbers.*

## 3.2 Transformation of directivity

To be able to interpret noise calculation results, the total sound pressure level from a blade section has to be related to an observer position. This is done by taking the directivity, that was explained in section 2.3, Figure 2-7, into account together with

the transformation of the position of the sound source into a global coordinate system.

The local e-coordinate system in Figure 2-7 is located at the airfoil section trailing edge line. The $x_e$-axis is aligned with the airfoil chord, with positive direction downstream from the trailing edge. The $y_e$-axis is aligned with the trailing edge, whereas the $z_e$-axis is perpendicular to the blade span.

A global coordinate system is defined at the position of the observer, at position 5 in Figure 3-1. The observer is placed at some height above the ground, $h_o$. The angle relative to the wind turbine upstream direction is, $\Theta_o$. The distance from the tower base center is, $r_o$.

The retarded distance, $r_e$ is found by transformation from coordinate system 1 to coordinate system 5. The directivity angles, $\Theta_e$ and $\Psi_e$ are then found by vector calculus in the global coordinate system 5.

The transformation is based on the 5 coordinate systems, whose positions are shown in Figure 3-1. They are respectively:

1. The e-coordinate system shown in Figure 2-7.
2. The lifting line.
3. The rotor center of rotation.
4. The tower base.
5. The observer position.

For each blade segment, the retarded observer distance, $r_{ei}$ is then calculated together with the directivity angles, $\Theta_{ei}$ and $\Psi_{ei}$.

The directivity for the leading edge is calculated in a similar manner with the local e-coordinate system located at the leading edge.

# 4 Noise prediction

This chapter contains the application and verification of the noise prediction model, described in chapter 2 and 3. There are two fundamental demands to the noise prediction model:

1. By absolute comparison of measurements and predictions of the total noise, it should be possible to obtain agreement within the uncertainty related to measurements, which is around 1.5 - 2 dB(A).

2. By relative comparison between different designs in the design phase, the prediction model should reveal the proper difference in the total noise.

Comparisons with measurements are carried out with for Danish wind turbines, the Vestas V27 225 kW and the Bonus Combi 300 kW. These are briefly described in Appendix A. The measurements were performed by Jacobsen and Andersen, reported in 1993 [13] and 1995 [14]. The sound pressure level is referenced to 20 μPa.

First, the calculation of the sound power level is explained since this is necessary for comparison with the available measurements. Next, the spectra for the different noise sources are calculated for both wind turbines. The model sensitivity to tripped boundary layer, trailing edge bluntness, turbulence scale and observer position for the sound pressure level is found. Comparisons with measurements of the total sound power level are made. The sensitivity of the rotor design to the noise emission is investigated for different wind speeds, tip pitch angles and tip speeds. Finally, the directivity of the sound pressure level around the Vestas V27 is mapped.

## 4.1 The sound power level

Standardized methods for noise measurements were recently proposed by IEC Ref. 88/48/CDV [11]. This standard is somewhat in agreement with the Danish departmental order for noise from wind turbines [12]. Measurements of the overall noise from wind turbines is normally achieved by using a hard board on the ground as foundation for a microphone device. This is located downwind from the rotor at some distance. The outcome of the measurement is a spectrum containing noise from the wind turbine together with contaminating background noise from the surroundings. The background noise is measured when the rotor is stopped, it is then subtracted, to obtain the corrected total noise.

The sound pressure level is dependent on the distance from the microphone to the rotor. To gain a uniform basis for comparison, the IEC Ref. 88/48/CDV recommends the calculation of the sound power level, $L_W$, for an equivalent single noise source at the rotor center:

$$L_W = (L_P)_{TOTAL,c} - 6 + 10\log\left(\frac{4\pi R^2}{S_0}\right) \qquad (4\text{-}1)$$

Where $(L_P)_{TOTAL,c}$ is the total sound pressure level corrected for back ground noise, -6 dB(A) is a correction for reflection from the hard board, $R$ is the distance from

the measurement observer point to the rotor center and $S_o$ = 1 m$^2$ is a reference area.
When the sound power level is calculated from the sound pressure level at some distance, measurements or predictions at different positions can be compared. For noise predictions, the correction for the microphone is omitted, since the calculation is unaffected by reflections. The sound power level is in the following calculated with reference to 1 pW.

## 4.2 Spectra for different noise sources

This section contains predictions of the spectra for the different noise sources for both wind turbines at 8 m/s. Figure 4-1 and Figure 4-2 show results for the Vestas V27 and the Bonus Combi, respectively. The overall impression of the spectra is a large degree of similarity. This is probably because the two turbines have points of resemblance, the most important being their almost similar size.

Characteristics for the different noise sources are summarized in the following:

Turbulent inflow noise is calculated under the assumption, that the turbulence length scale is 100 m and independent on height, though this is a rather crude simplification [5]. The turbulence intensity is 0.1, which is close to the Danish Roughness Class 1. The turbulence intensity is defined as the root mean square of the turbulent velocity divided by the mean wind speed.

The spectrum is broadband and shows an area of high power at low frequencies. It is then reduced towards higher frequencies. Since the power level is high over a large part of the total spectrum, the choice of turbulence parameters is essential for a correct prediction of the total noise. These parameters are however connected with large uncertainties. The importance of the length scale is therefore further investigated in section 4.3.

Noise from turbulent trailing edge flow is divided into contributions from the pressure and the suction side together with separation noise, that origins from the angle of attack and possible flow separation. It is assumed that the flow is untripped at the airfoil leading edges along the blade span rather than tripped. Noise from the pressure side is broadband with maximum power around 2500 Hz. Noise from the suction side together with noise from separation/ angle of attack is broadband with maximum power around 800 Hz and 500 Hz for the Vestas V27 and The Bonus Combi, respectively. The noise prediction model is based on experiments in a wind tunnel environment with low background turbulence. Tripped and untripped flow are two ideal different cases. It is likely that measurements in natural conditions would fall in between because of higher background turbulence and increased surface roughness. The effect of tripped versus untripped flow is therefore further investigated in section 4.3.

Laminar boundary layer vortex shedding noise results in a rather narrow band with two peaks from tonal noise. Tonal noise was reported from wind turbines in natural conditions. However, prediction is far more complicated than the proposed model, that is build upon the ideal wind tunnel environment. Neither the Vestas V27 nor the Bonus Combi measurements reveal any signs of laminar vortex shedding noise. Therefore, the contribution from this source was neglected in the total noise calculation.

Noise from trailing edge bluntness is calculated by estimating the thickness of the trailing edge to some percentage part of the chord. For both turbines, 0.5% is used.

This gives a maximum thickness of around 6 mm. The spectrum is rather narrow band and has a peak around 2500 Hz. This peak is however dependent on the trailing edge thickness. The estimate of a proper thickness is difficult without detailed knowledge of the blades on the measured rotor. The airfoil shape towards the trailing edge is believed to influence the radiated noise. Hence, the influence from differences in trailing edge thickness will be investigated in section 4.3. Noise from trailing edge bluntness is of minor importance to the total noise and because of the uncertainty of the trailing edge thickness, the total noise is calculated without the contribution from trailing edge bluntness.

The tip noise is rather broadband with peak frequency around 1600 Hz. The maximum power level is below the other noise sources. It therefore appears that this noise source is of minor importance to the total noise, though it might have some importance at higher tip speeds. This finding concerning the model of Brooks, Pope and Marcolini [1], is consistent with findings in [4].

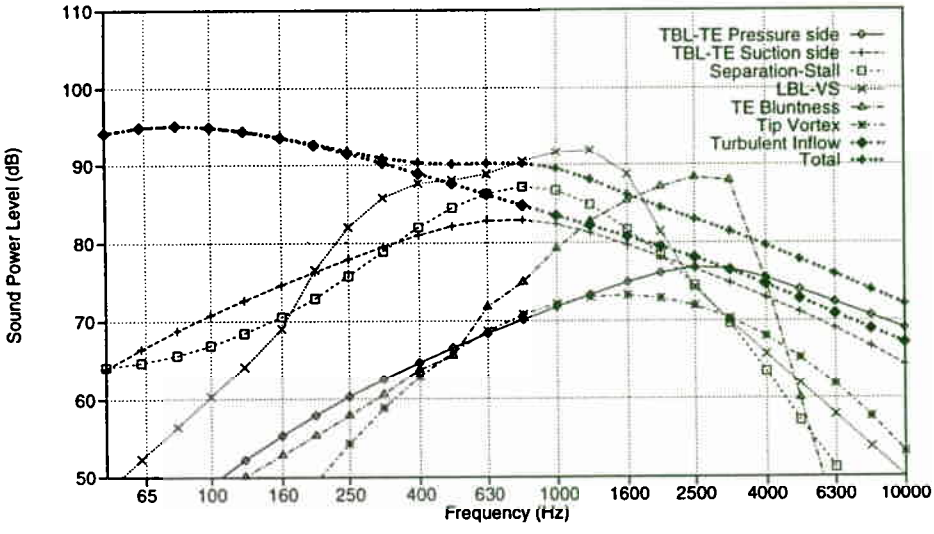


*Figure 4-1* *Spectra for airfoil self noise and turbulent inflow noise in dB for the Vestas V27 at 8 m/s, tip pitch 0.5°.*

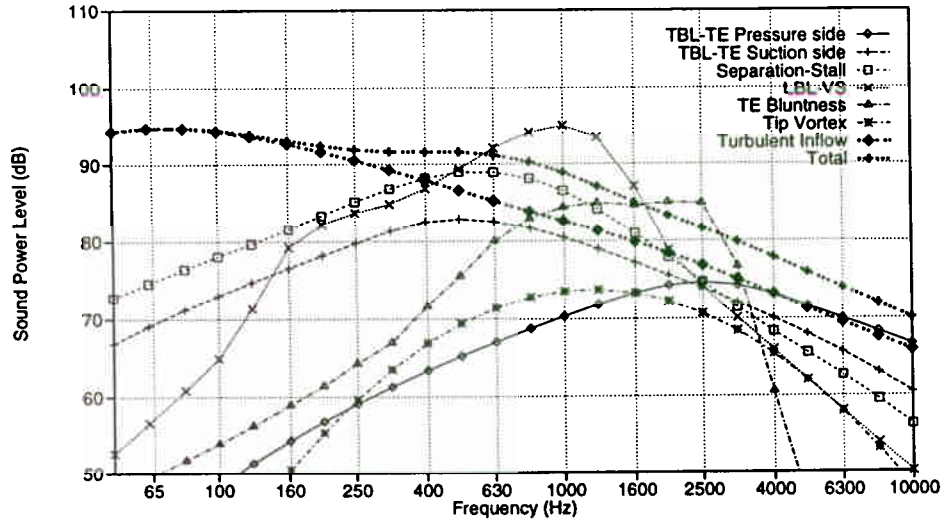


*Figure 4-2* *Spectra for airfoil self noise and turbulent inflow noise in dB for the Bonus Combi 300 at 8 m/s from.*

Finally, the total noise in dB is calculated without contributions from laminar vortex shedding trailing edge bluntness. At low frequencies, the turbulent inflow noise dominates the frequency spectrum. At intermediate frequencies, trailing edge noise together with turbulent inflow noise are the most significant sources. If laminar vortex shedding noise and blunt trailing edge noise are included they will lead to local peaks in this area of the total spectrum. At high frequencies, turbulent trailing edge noise dominate together with turbulent inflow, whereas tip noise contributes only with a minor part. All in all, turbulent inflow seems to be of major importance to the overall noise together with turbulent trailing edge noise.

## 4.3 Model sensitivity analysis

In this section, the sensitivity of the predicted noise spectra is investigated to changes in the input parameters. The purpose is to put up a number of guide lines when the noise prediction model is being used. Either at the design stage, when the rotor blades are being designed, or when noise predictions are compared to measurements, to gain knowledge of the different noise sources defining the total noise.

The following points are investigated:

- The difference between tripped and untripped flow
- The effect of trailing edge bluntness
- The effect of turbulence length scale
- The observer distance from the rotor.

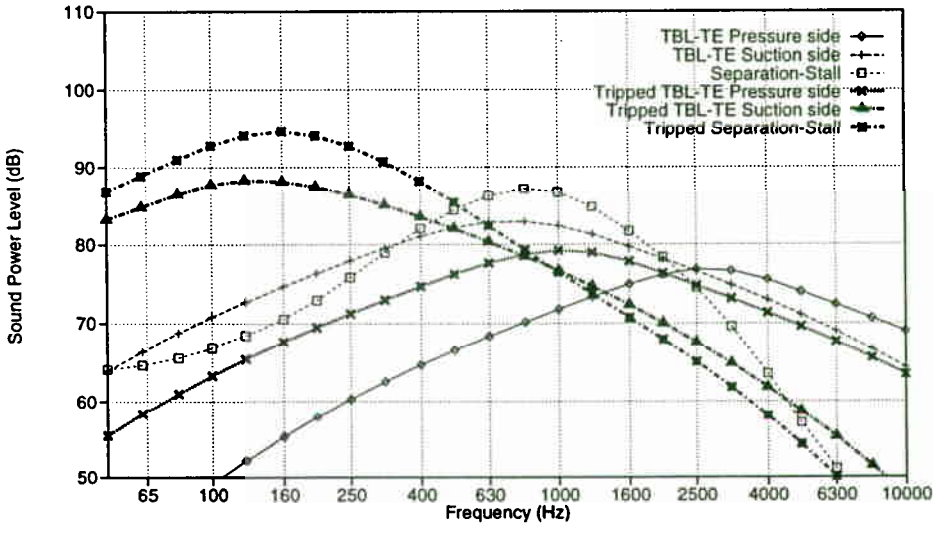


*Figure 4-3* *Untripped/ tripped turbulent boundary layer trailing edge noise for the Vestas V27, Wind speed 8 m/s, Tip pitch angle 0.5°.*

**Tripped boundary layer**

Figure 4-3 shows the predicted noise spectrum from turbulent flow at the trailing edge with either untripped or tripped flow for the Vestas V27 at 8 m/s. The main tendency is a shift toward lower frequencies for the peak power frequency. In addition, the maximum power is increased. The shift in frequency will affect the total noise spectrum, so that energy will be transferred to lower frequencies.

The operational conditions for wind turbines are very different, and difficult to foresee, when erecting turbines on new sites. The design stage should therefore contain noise calculations at both tripped and untripped flow. When comparisons are carried out with measurements, the condition that suits the measurements best should be chosen.

### Trailing edge bluntness

Figure 4-4 shows the noise spectrum from trailing edge bluntness for the Bonus Combi 300 kW for different values of the trailing edge thickness. An increase in trailing edge thickness can lead to a significant increase in maximum power and a shift in the peak frequency towards lower frequencies. Since the importance of the trailing edge noise will rely on the finish of the blade trailing edge rather than on the blade layout itself, it is difficult to predict the trailing edge noise already in the design phase, before the blade is actually being manufactured. Therefore the trailing edge bluntness should then be omitted in the calculation of the total noise. When comparing to measurements, the trailing edge bluntness noise should be omitted if the measured spectrum does not show any peak, that could origin from this noise source.

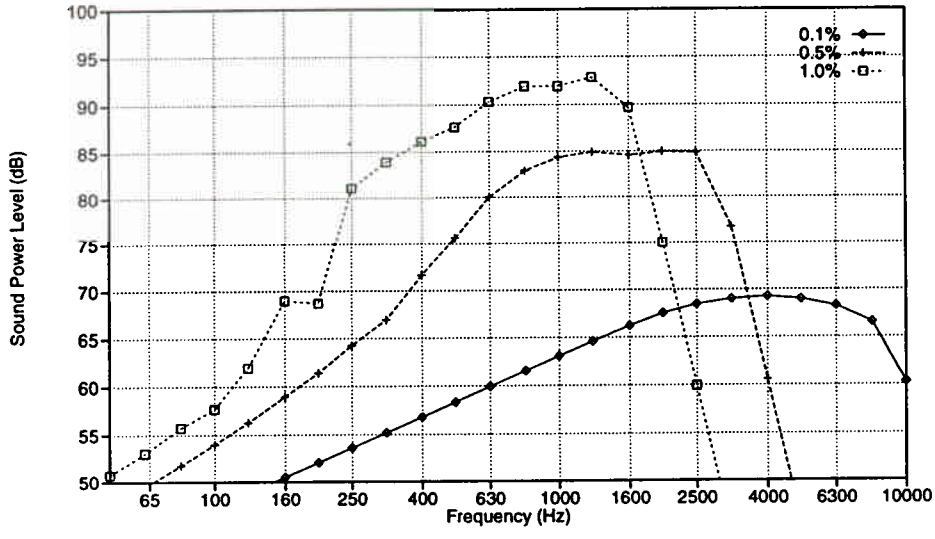


*Figure 4-4* *Noise from trailing edge bluntness for the Bonus Combi 300 kW, The trailing edge thickness is given in percent of the chord.*

### Turbulence length scale

The predicted noise spectrum from turbulent inflow is shown for the Bonus Combi 300 kW, for different turbulence length scales, in Figure 4-5. It can be seen, that the shape of the spectrum is nearly unaffected by the change in turbulence length scale, whereas the power level is increased with higher length scale. It is obvious, that correct turbulence properties are crucial to a correct prediction of the total noise, since the turbulent inflow noise is of major importance. The turbulence length scale is however a very complex parameter to determine, since it depends on the specific site and the climate. It is a topic of international research, that has not yet been sufficiently resolved. It is important, that the order of magnitude for the noise from turbulent inflow is correct, since this determines the importance of the airfoil self noise. At the design stage, the total noise should always be split into noise from turbulent inflow and airfoil self noise, so that the airfoil self noise is not neglected because of too high noise from turbulent inflow.

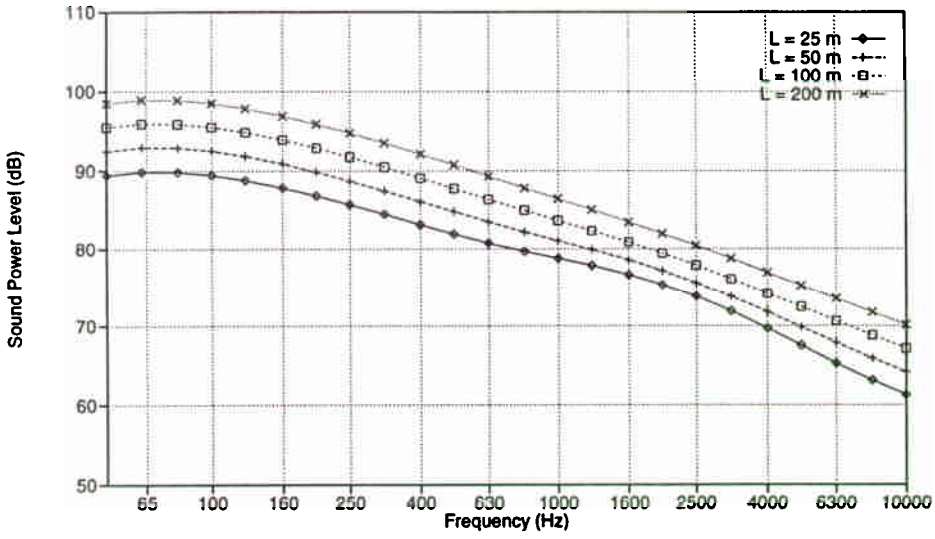


*Figure 4-5* *Noise from turbulent inflow for different turbulence length scales for the Bonus Combi 300 kW at 8 m/s.*

### Observer distance for prediction

The prediction of the sound pressure level is related to the distance between the observer and the emitting noise sources. When results from different measurements/ predictions are compared, the influence from the distance is accounted for by calculating the sound power level from eq. (4-1). In Figure 4-6, the predicted total sound power level is shown as function of the distance from the observer to the rotor. Though the sound power level is not constant, the variation is minor and it can be concluded, that the distance is not important. However, when measurements are compared with predictions, the distance could just as well be chosen identical to the measurement.

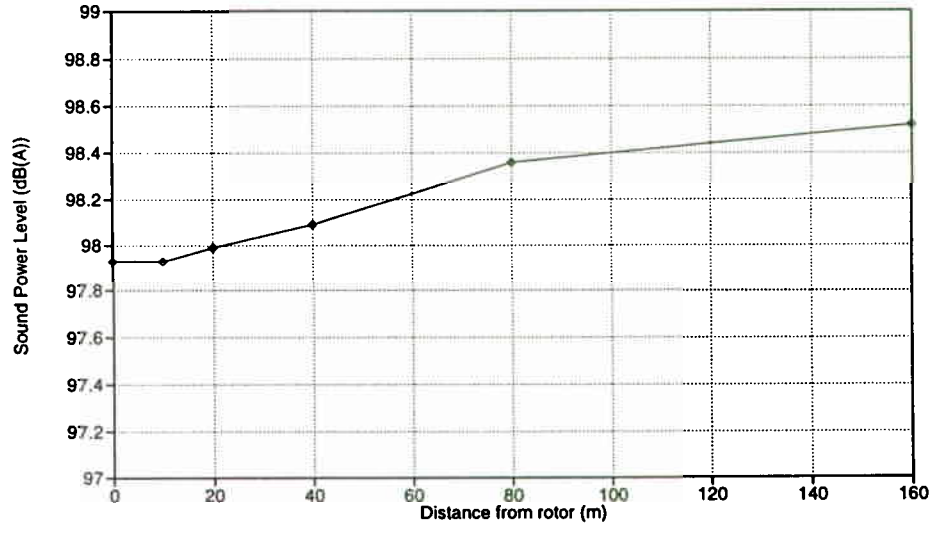


*Figure 4-6* *Sound Power Level in dB(A) versus calculation distance downstream from the rotor for the Vestas V27 at 8 m/s, tip pitch 0.5°*

## 4.4 Comparison with experiment

In this section, predictions of the total sound power level are compared to measurements carried out by Jacobsen and Andersen [13] [14]. The measurements were performed according to IEC 88/48 CDV. The wind speed for comparison is chosen to 8 m/s.

The predictions are performed from the guidelines found in section 4.3. The turbulence length scale is 100 m. Noise from laminar vortex shedding and blunt trailing edges is omitted. Calculations are performed with both tripped and untripped flow. The distance from the rotor is 40 m downstream from the tower center, at the ground level. Resulting sound pressure levels are converted to the equivalent sound power level for a single source in the rotor center.

Predictions and measurements of the total A-weighted sound power level for the Vestas V27 with tip pitch 0.5° are shown in Figure 4-7. In general, there is good agreement. The measurements show no signs of tonal frequencies from the machinery, laminar vortex shedding or trailing edge bluntness. The difference between untripped and tripped flow is seen to shift the spectrum towards left, as previously noticed. At low frequencies, the untripped prediction seems to fit best, whereas the tripped prediction is better suited at the higher frequencies. The total sound power level is calculated to 98.1 dB(A) for untripped flow and 97.1 dB(A) for tripped flow. The measurements show 97.5 dB(A) [13]. The deviation is within the range of uncertainty of 1.5 dB(A) on the experimental data [13]. Even though the shape of the spectrum is affected by the flow condition, the total predicted noise is sufficiently accurate.

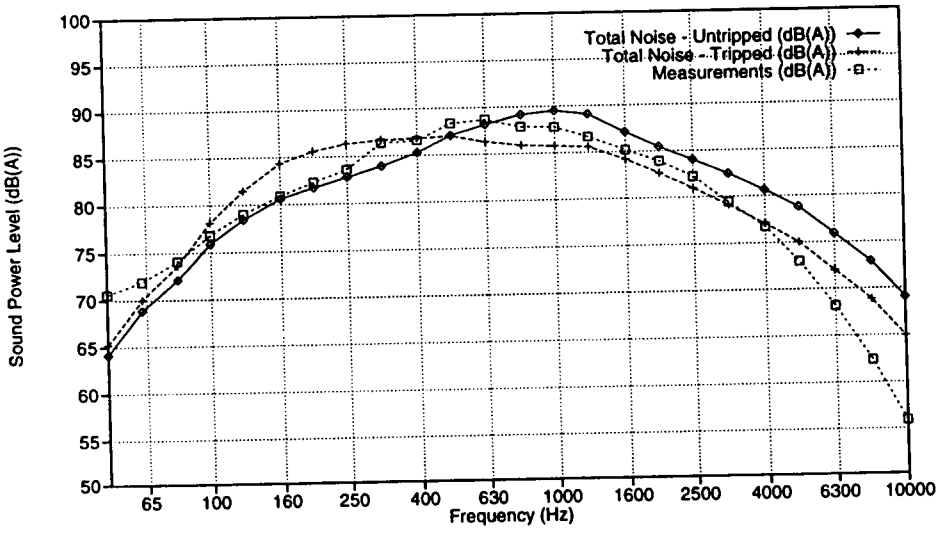


*Figure 4-7* *Predicted sound power level in dB(A) compared to experimental results from Jacobsen & Andersen [14] for the Vestas V27 wind turbine at 8 m/s, tip pitch 0.5°.*

Figure 4-8 shows predictions and measurements for the Bonus Combi 300 kW. Good agreement is again found. The measured spectrum reveals two tonal areas. At 250 Hz, there is a significant peak. This was investigated in [13], and was found to originate from machinery noise. At 2000 Hz there is a minor irregularity in the spectrum shape. This could be either due to tip noise or blunt trailing edge noise.

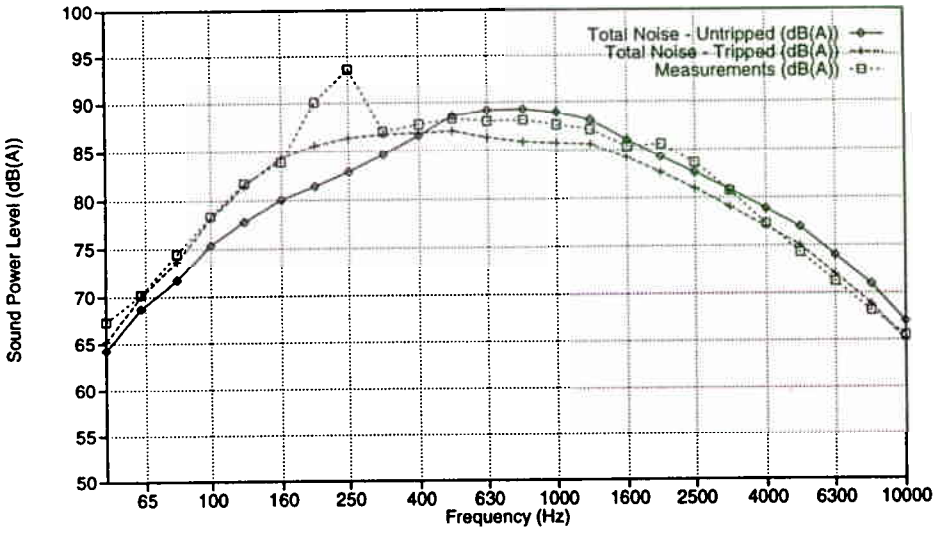


*Figure 4-8* *Predicted sound power level in dB(A) compared to experimental results from Jacobsen & Andersen [13] for the Bonus Combi 300 kW wind turbine at 8 m/s.*

The predictions show the same trend, as it was found for the Vestas V27. At low and high frequencies, the agreement between the tripped prediction and the measurements is best, whereas the untripped prediction is best suited at intermediate frequencies. The total sound power level is found to 98.0 dB(A) for the untripped prediction, 97.1 dB(A) for the tripped prediction compared to 99.1 dB(A) for the measurements without the tonal contribution from machinery. Again the agreement is satisfactory.

Apparently even better agreement on the spectrum shape could be obtained by fitting the turbulent trailing edge noise and the turbulent inflow noise to the measurements. However, this is of minor importance, since the deviation is already equal to or below the measurement accuracy.

It appears that the predictions of the two wind turbines are almost identical regarding the total sound power level. This is mainly because they have a large degree of similarity regarding rotor diameter, tower height and tip speed.

## 4.5 Design sensitivity analysis

In the previous section, it was found that the prediction model was sufficiently accurate in two cases. However, the simplicity of the model implies that this is probably not always the case. An accurate prediction is of course important, but more detailed modeling together with further experimental work is needed to improve the present model significantly. However, a relative basis for comparison of different rotor designs is very important in the design phase, regarding their total noise emission. The purpose with this section is to investigate the total sound power level variation with wind speed, tip pitch angle and tip speed, to be able to compare different rotors at different operational conditions.

### Wind speed variation

The noise is predicted at different wind speeds for the Bonus Combi 300 kW. Figure 4-9 shows the different spectra. Apparently, the variation with wind speed is large for low frequencies, whereas the higher frequencies are almost unaltered.

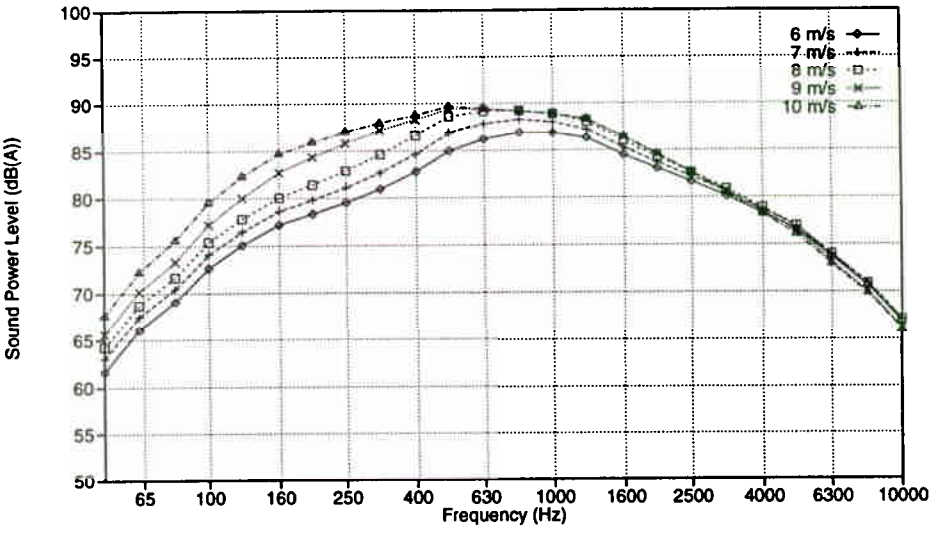


*Figure 4-9* *Total noise spectrum predicted at different wind speeds for the Bonus Combi 300 kW.*

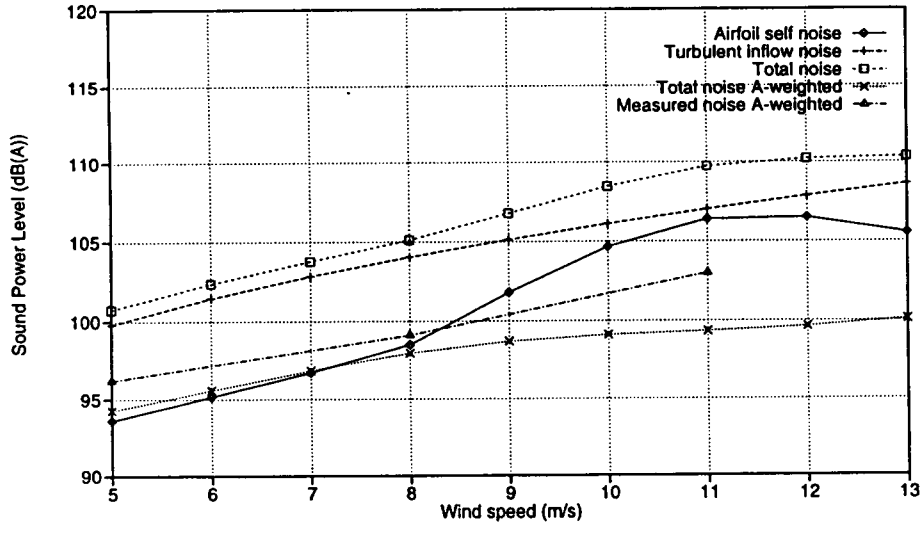


*Figure 4-10* *Total sound power level versus wind speed for the Bonus Combi 300 kW.*

Figure 4-10 shows the predicted sound power level versus wind speed compared to measurements. As expected, the total sound power level is increased with wind speed. The measurements are extrapolations from results mainly around 8 m/s. Hence, they are less accurate at low and high wind speeds. However, there is good agreement at low wind speeds, whereas the prediction tend to bend off at higher wind speeds. The offset, that was found in the previous section remains constant at low wind speeds.

The total noise is divided into noise from turbulent inflow and airfoil self noise. It can be seen, that noise from turbulent inflow is dominating the total noise especially at low wind speeds. This implies, that changes in the airfoil self noise will have only little effect on the total noise. Further work should therefore clarify, whether the relation between the levels of the two noise sources is correct.

### Tip pitch angle variation

The noise is predicted for different tip pitch angles for the Vestas V27. The different spectra are shown in Figure 4-11. It appears, that they differ at intermediate frequencies around 400 -1600 Hz. Since the noise from turbulent inflow remains constant, a change in the airfoil self noise causes the variation.

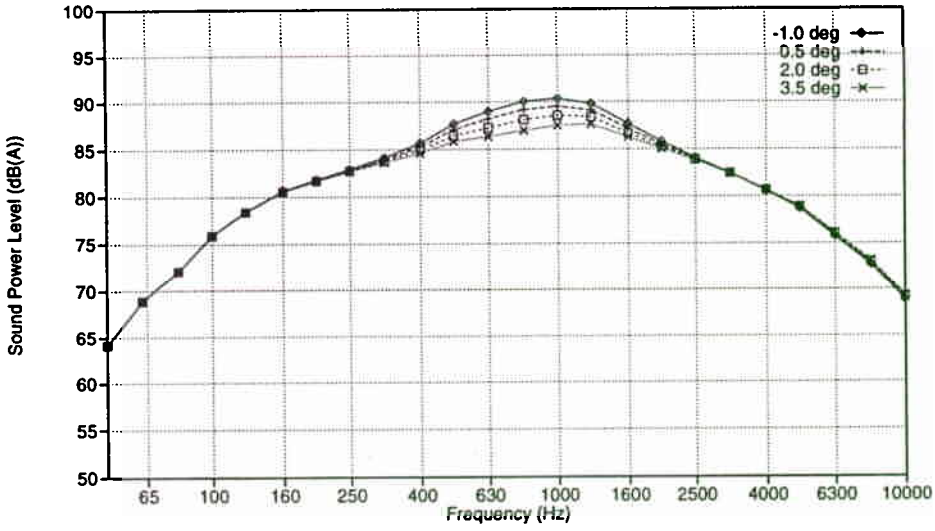


*Figure 4-11* *Total noise predicted for different tip pitch angles, compared with experiment for the Vestas V27 at 8 m/s.*

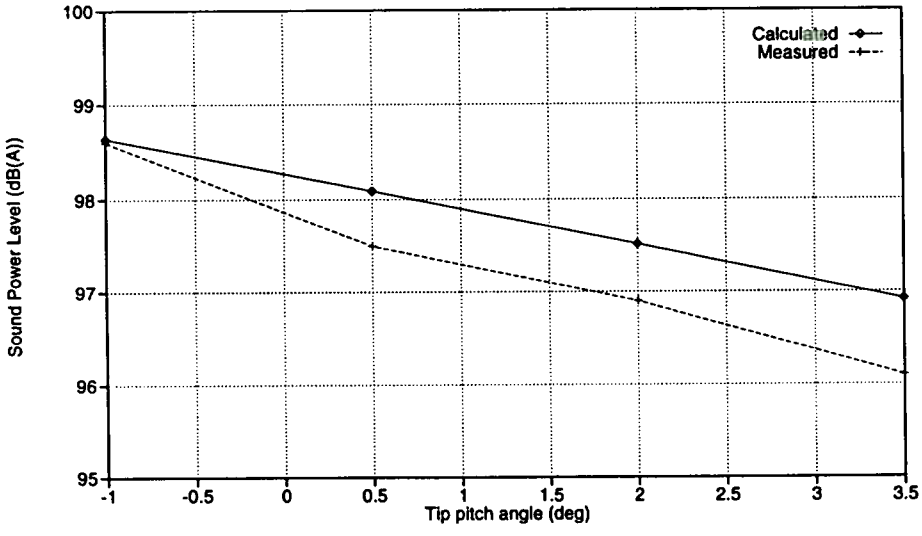


*Figure 4-12* *Sound power level in dB(A) predicted for different tip pitch angles, compared with experiment for the Vestas V27 at 8 m/s.*

Figure 4-12 shows the total predicted sound power level versus tip pitch angle, together with measurements. The measurements show a slightly steeper reduction in noise when the tip pitch angle is increased, but in general there is a fair agreement.

The agreement with measurements indicates, that the weighting between the noise from turbulent inflow and airfoil self noise seems to be valid. Even though the dominating noise from turbulent inflow remains constant, the total noise is being reduced when the tip pitch angle is increased. This is because the airfoil self noise

is reduced in the intermediate frequency range. The A-weighting influence is minor in this frequency area, and the reduction is therefore seen on the total noise.

### Tip speed variation

The noise is predicted for the Bonus Combi 300 kW at different tip speeds. Unfortunately, measurements have not been available. Instead, an empirical expression by Wolf [15] was used for comparison:

$$L_{WA} = 10\log D + 50\log v_t - 4 \qquad (4\text{-}2)$$

Where $v_t$ is the tip speed.

Figure 4-13 shows the frequency spectra for different tip speeds. There appears to be a large variation in the power level with tip speed over the entire frequency range, especially at high frequencies. This is partially because of the contribution from tip noise, where the peak frequency is shifted toward higher frequencies at higher tip speeds, whereas the maximum power level is practically unchanged. However, turbulent inflow noise and airfoil self noise are in general increased with tip speed.

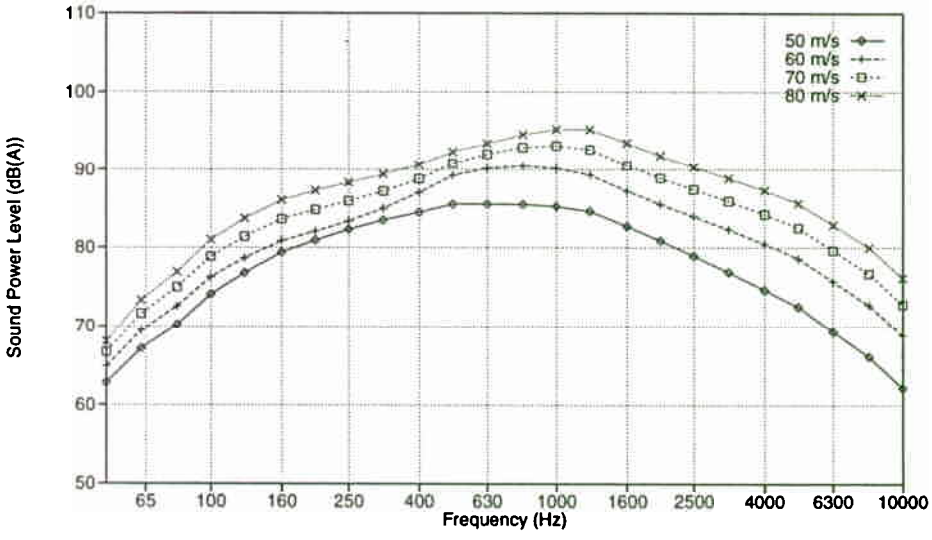


*Figure 4-13* *Total noise predicted at different tip speeds for the Bonus Combi 300 kW.*

The total sound power level is shown in Figure 4-14. Even though the empirical eq. (4-2) is very simple, there is good agreement. At higher tip speeds, the total noise seems to be over predicted by eq. (4-2). There is a linear increase in the noise from turbulent inflow, whereas the airfoil self noise tend to increase mainly at lower tip speeds. Even though the total sound power level is dominated by the noise from turbulent inflow, airfoil self noise is again seen to be an important contribution.

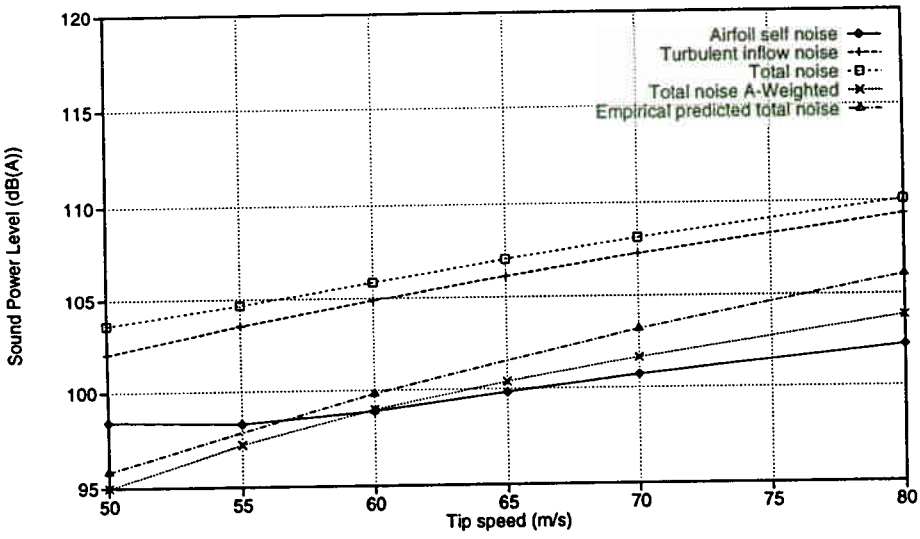


*Figure 4-14* *Sound power level in dB(A) versus tip speed for the Bonus Combi 300 kW.*

## 4.6 Directivity

The purpose with this section is to validate the directivity that was applied to the airfoil trailing edge in Chapter 2 and 3.

When the rotor azimuth angle is changed, the directivity of the radiated noise is changed. This is due to the change of distance and angle from the observer to the noise sources. However, measurements carried out following the IEC ref. 88/48/CDV recommendation are averaged in 2 min. This means that azimuth variations of the directivity are averaged. Thus, there is no need for an investigation of the noise as function of the rotor azimuth angle.

When the position of the observer is changed, there is also a change in directivity. To investigate the sound pressure variation with the observer position, a number of predictions is performed. The observer distance on the ground level is changed together with the observer angle, relative to the wind turbine upwind direction. Figure 4-15 shows contour levels of the total sound pressure level for the Vestas V27 at the ground level plane. The downstream direction corresponds to the y-axis towards positive, whereas the x-axis is the horizontal position in a plane aligned with the plane of rotation. The rotor is located in the origin and rotating clockwise when looking in the downwind direction.

It can be seen that the sound pressure level at some constant distance to the tower center is changing with observer angle. The sound pressure level is maximum in the upwind and downwind directions, whereas the sound pressure is lower in the plane of rotation. This is consistent with measurements reported by Hubbard and Shepherd [16]. They reported that the nature of the noise radiation pattern for low frequency rotational noise components show a radiation picture similar to a dipole. At higher frequencies, the radiation picture is still oval. Hence, the overall radiation picture is in well agreement with the prediction. It should be noted that the prediction does not include the sound propagation in the viscous earth boundary layer.

It can furthermore be seen that the radiation picture is slightly skewed counter clockwise in the plane of the paper, probably from the direction of rotation.

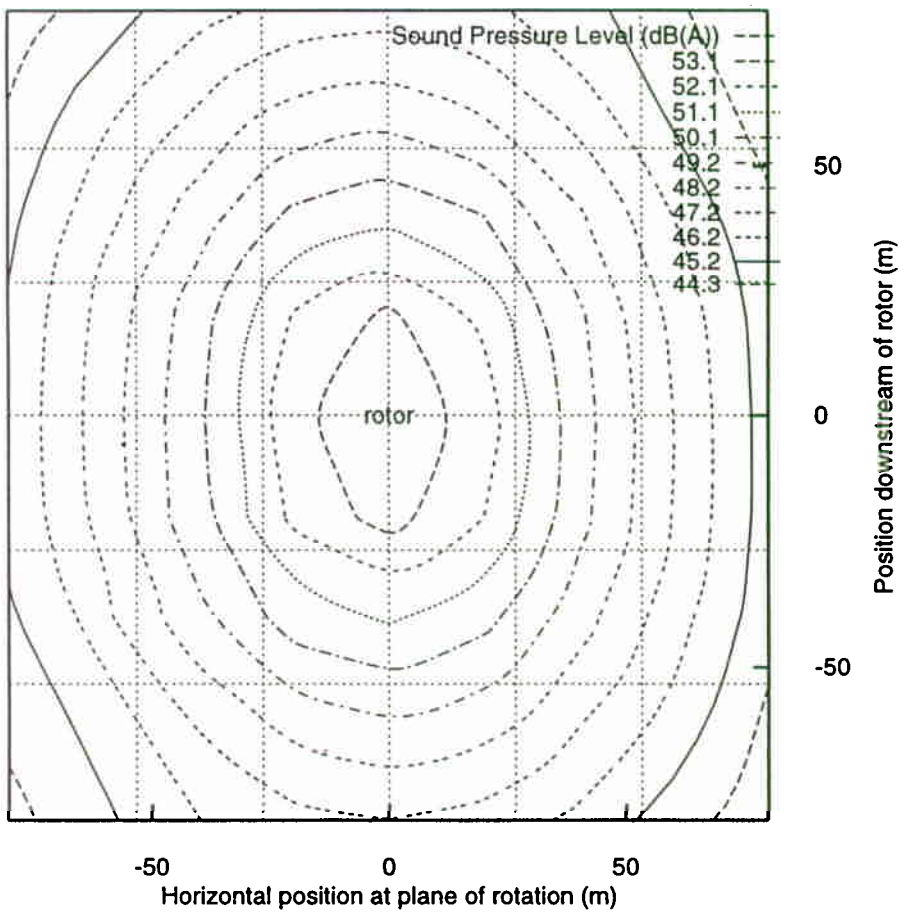


*Figure 4-15* *Contour plot of sound pressure level around the Vestas V27 wind turbine. The downstream direction corresponds to the y-axis towards positive. The x-axis corresponds to the plane of rotation. The rotor is located in the origin and rotating clockwise, when looked on in the downstream direction.*

## 4.7 Summary

The key results from this chapter are summarized in the following:

The different noise sources from airfoil self noise and turbulent inflow noise were investigated and it was found, that the turbulent inflow noise is dominating in most of the frequency range. However, turbulent trailing edge noise is also important.

Laminar boundary layer vortex shedding noise was not found in the measurements, and was not included in the predictions of the total noise. It was also found difficult to include blunt trailing edge noise because of missing information about the details of the trailing edge design.

A sensitivity analysis on the model parameters was performed. It was found important to investigate both untripped an tripped flow, since a turbine in natural conditions may not entirely have any of these conditions. Turbulent inflow noise is sensitive to the input turbulence parameters, that are connected with large uncertainties. The total noise should therefore be split into turbulent inflow noise and airfoil self noise to reveal the airfoil self noise.

Comparisons with measurements of the total noise spectrum showed sufficient accurate values of the total sound power level, within a range of 2 dB(A). Furthermore the relative variation of the total sound pressure level with the important parameters: wind speed, tip pitch angle and tip speed was verified with experiments and empirical predictions. Even though there is a small absolute deviation, the relative variation with each parameter was found in good agreement. This is important for design purposes, where different designs can be judged by their relative total sound power level.

Noise from turbulent inflow was found to dominate the total predicted noise. There is a risk of hiding the airfoil self noise contribution. However, by the variation of the pitch angle, the turbulent inflow contribution remained constant, while a drop in the airfoil self noise ensured good agreement. Furthermore the agreement with both wind speed and tip speed indicates that the relation between turbulent inflow noise and airfoil self noise is correct. Therefore, the prediction model is usable even though the magnitude of the sound power level from the different noise sources might not be entirely correct.

The directivity of the total sound pressure level with the observer on the ground distance and angle was investigated and found in qualitative agreement with measurements.

Future work should involve the airfoil contour, since the present model is simple regarding the degree of detail with respect to the airfoil contour and the noise mechanisms.

# 5 Rotor optimization with noise considerations

This chapter contains a design study for development of new blades for the Bonus Combi 300 kW. The aim is to be able to control the total noise emission in the design process by use of the noise prediction model together with a design tool based on mathematical optimization. The used design tool, "ROTOR", was developed at Risø and is further described in [7].

First, the design tool is briefly described. Then, three different design studies are carried out. These concern either noise minimization or noise constraining. They are compared and main tendencies are revealed. At the end it is discussed how well suited the present noise prediction model is for application with the design tool.

## 5.1 Optimization design tool

The optimization tool, "ROTOR", uses a mathematical optimization algorithm in connection with a number of calculation models for calculation of the rotor aerodynamics, blade structure, extreme/ fatigue loads and cost. The designer specifies an initial design, that is an initial guess on a rotor design. Furthermore an objective function is specified. The objective function expresses the aim of the optimization. This could be e.g. maximum annual production, minimum noise emission or minimum cost. In addition, a number of design variables are specified. The design variables are chosen among the blade geometry, such as chord, twist and the operational conditions, e.g. tip speed. Finally constraints are added. The constraints bound the possible solution into a feasible region. Constraints can be applied to loads, generator power, blade strains and so on.

The optimization algorithm finds an optimum design in a systematic and automatic way by use of the different calculation models. In this process, the design variables are changed within the bounds from the constraints to yield a minimum value of the objective function.

After the optimization, the designer performs control calculations of the result. Eventually smaller justifications or a reformation of the optimization problem is performed.

The most significant advantages by use of systematic optimization instead of the "manual" changes by the designer is, that a large number of parameters (design variables) can be varied simultaneously. Furthermore, an unlimited number of constraints are automatically being fulfilled by the optimization algorithm. A disadvantage is the iterative procedure, that can involve long calculation time, especially when the individual calculation models are time consuming, since the algorithm is based on numerically differentiation of the objective function and the constraints.

## 5.2 Rotor optimization

Three different optimizations studies are performed according to the following problem setup:

1. The first study concerns a rotor where the total aerodynamic noise from the rotor is minimized subject to constraints on the minimum allowable annual production and the maximum generator power. Both the annual production and the generator size are in this way kept equal to the Bonus Combi 300 kW.

2. The second study concerns a rotor where the annual production is maximized subject to constraints on the maximum noise and the maximum generator power. The noise emission and the generator size are then kept equal to the Bonus Combi 300 kW.

3. The third study concerns a rotor where the production is maximized with constraint on the maximum generator power, but no considerations on noise.

Design variables are the blade chord and twist distributions together with the tip pitch angle and the tip speed. The airfoil shape and the blade relative thickness together with the rotor diameter remain unchanged. There are no constraints on loads, since the primary interest is the aerodynamic properties. This could cause problems with the resulting blade design, especially in the root section, where both the optimum chord and twist tends to be large [7]. Therefore, the blade maximum chord and the maximum twist are constrained and the tip chord is kept constant to ensure the relevance of the results. Furthermore, the tip twist is fixed to zero by convention.

The wind climate is chosen as Danish roughness class 1, according the Danish Code of Practice for Wind Turbines [10].

When comparing noise levels with the Bonus Combi 300 kW, the predicted value will be used to avoid the offset on the absolute value found in the previous chapter.

*Table 5-1* *Overall results for the three different optimized rotors, compared to the Bonus Combi 300 kW.*

| | Bonus Combi 300 kW | 1) Optimized for min. noise constrained production | 2) Optimized for max. production constrained noise | 3) Optimized for max. production |
|---|---|---|---|---|
| Production (MWh) | 838 | 838 | 855 | 860 |
| Noise (dB(A)) | 98.0 | 94.9 | 98.0 | 101.2 |
| Tip speed (m/s) | 56.8 | 50.1 | 57.0 | 65.2 |
| Tip pitch (deg) | -1.8 | 1.2 | 0.8 | 0.6 |

Key results are shown in Table 5-1. The resulting chord and twist distributions are shown in Figure 5-1 and Figure 5-2 respectively. The power curve versus wind speed is shown in Figure 5-3.

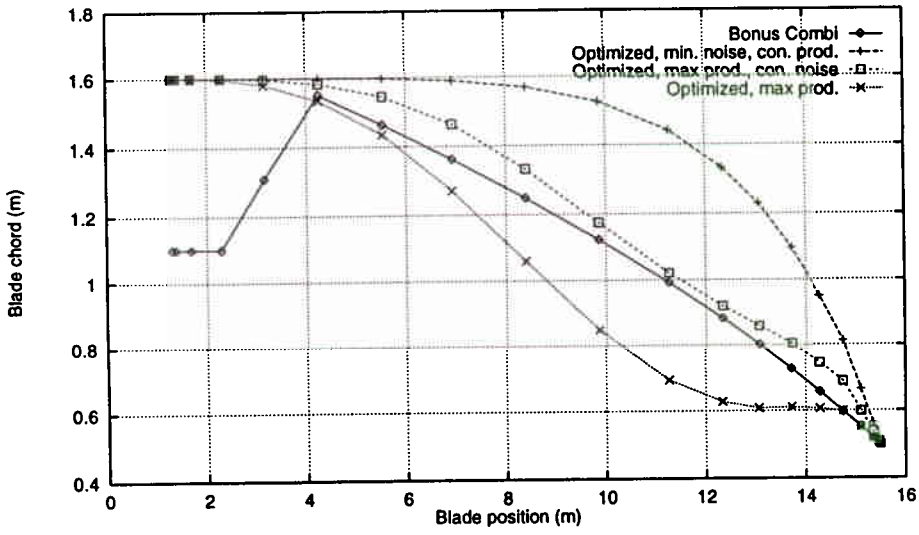


*Figure 5-1* *Chord distribution for the Bonus Combi 300 kW and the optimized rotors for minimum noise and maximum production, respectively.*

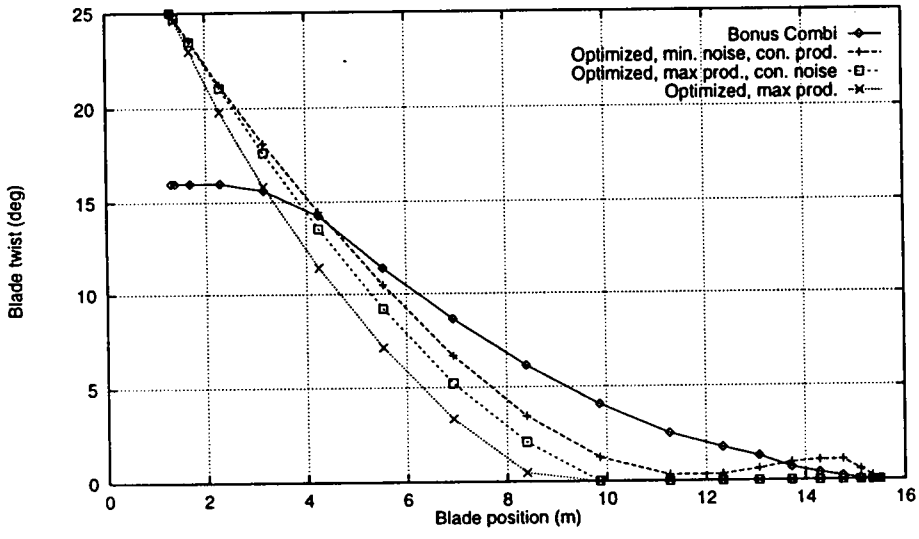


*Figure 5-2* *Twist distribution for the Bonus Combi 300 kW and the optimized rotors for minimum noise and maximum production, respectively.*

**1) Optimization study for minimum noise**

It appears from Table 5-1, that the first optimization has resulted in a rotor, that has equal peak power and annual production as for the Bonus Combi 300 kW. The total sound power level is minimized to 94.9 dB(A). This is a substantial reduction, since a drop in around 3 dB(A) corresponds to a halving of the sound power.

Overall parameters of importance for the reduction of the noise are the drop in tip speed to 50.1 m/s. This decreases the airfoil free stream velocity along the blade span. Furthermore, the tip pitch angle is increased to 1.2°. This decreases the angle of attack and delays the stalling of the blade until a higher wind speed, so that peak power is attained. In addition, the noise from the trailing edge will be reduced from the drop in angle of attack, since this is of major importance to most noise sources.

The blade design is changed so that the chord is increased over most of the blade (Figure 5-1). This is necessary to maintain the peak power and the annual production, because the tip speed is reduced. The twist is reduced on a large part of the blade, resulting in an increase in the angle of attack (Figure 5-2). However, at the tip this increase is counter balanced by the increase in tip pitch and the resulting angle of attack is reduced. On the power curve in Figure 5-3, it can be seen, that the power is reduced just before rated power. This is counter balanced by an increase at wind speeds around 10 - 13 m/s, so that the annual energy production is maintained.

The resulting blade has a larger solidity and hence, more body in the swept area compared to the Bonus Combi 300 kW blade. The blade projection in a plane perpendicular to the extreme wind speed is increased This will result in larger extreme loads from rotor stand still at extreme wind speeds. Therefore, the strength of the blade should be increased by applying additional material. In addition, the tower and the foundation should be increased. Because of the lower tip speed, and hence, the lower angular velocity, the applied torque on the rotor shaft is increased. This results in a larger main shaft/ gearing. In addition, the moment from gravity on the hub from a blade will increase because of heavier blades. All in all, the wind turbine with the optimized rotor would be more costly. In fact, optimizations for minimum cost have shown results, somewhat in contrary to this. A more slender blade will result in less loads and hence, less cost for the entire wind turbine, since both fatigue damage and extreme loads are reduced.

The optimization result shown gives an idea about the trend in design parameters when the noise is reduced. In order to include noise aspects in this type of optimization, the economic value of noise reduction must be settled. It is however clearly demonstrated, that noise concerns can be included in the design process. The mechanisms in reduction of noise is a low tip speed combined with smaller angles of attack, especially at the tip. The optimum values for these should in a further study be looked for by evaluating the cost of additional noise, and comparing this to the overall cost of the wind turbine.

**2) Optimization with constrained noise**

The second optimization results in a rotor of equal noise emission and rated power as for the Bonus Combi 300 kW, but with maximized annual production. The annual production is increased by 2.0%, which is a very common value from aerodynamic optimization of an already existing blade, when the diameter is fixed [7]. The tip speed is slightly increased to 57.0 m/s, and the tip pitch angle is increased to 0.8°. Apparently, the influence on the noise emission from the increase in tip speed is counter balanced by the increase in tip pitch angle and the change in blade shape.
Compared to Bonus Combi 300 kW, the chord is slightly increased (Figure 5-1), whereas the twist is reduced (Figure 5-2). Hence, the angle of attack is increased, except for the tip region, where it is decreased. Hereby, the wind speed for rated power is reduced. This can be seen in Figure 5-3, where the power curve shows an increased power before the wind speed of maximum power.

All in all, the resulting blade is not too different from the Bonus Combi 300 kW, but fine adjustment of the blade chord and twist has resulted in a controlled increase of the annual production. The cost of the optimized blade is probably not very different from the starting point.

The optimization result indicates that constraining the noise emission could be a possible way to include noise concerns in the design process. It is probably difficult to assign cost to a certain sound power level. The maximum allowable noise emission is however given in departmental orders or regulatives. By the design of rotors to specific sites, these limits could be incorporated in the design process by application of the noise prediction model together with the design tool. However, this demands for a further increase in the degree of detail for the prediction model, to ensure a correct predicted level of the sound power.

### 3) Optimization with unconstrained noise

The third optimization is performed mainly for reference, since it does not contain any noise concerns. The annual production is maximized with constraint only on the maximum power. The resulting annual production is increased by 2.6% compared to the Bonus Combi 300 kW. The noise is hereby increased to 101.2 dB(A). This is mainly because of the increase in the tip speed to 65.2 m/s, whereas the tip pitch angle is increased to 0.6° (Table 5-1).

Compared to the Bonus Combi 300 kW, the chord is substantially reduced (Figure 5-1) and the twist is also reduced (Figure 5-2). The reduction in chord is necessary for not exceeding rated power, because the tip speed is increased. The power curve is somewhat in agreement with the result of the second optimization (Figure 5-3).

There is only a small increasé in the annual production compared to the second optimization. With the large increase in the sound power level, it can be concluded, that the aerodynamic optimum is very expensive in additional noise. This means, that the noise should always be constrained in the design process, either by application of the noise prediction model, or by constraining the tip speed, since this is the far most important parameter.

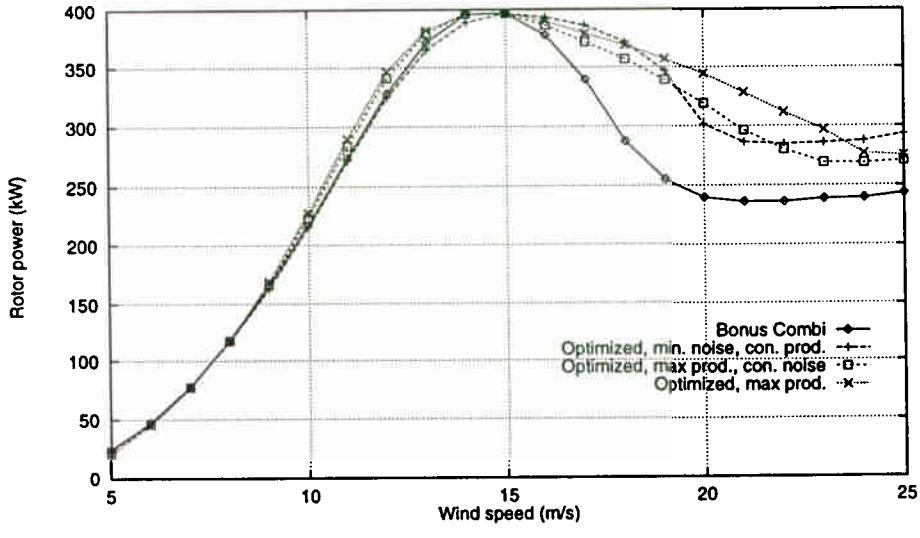


*Figure 5-3* *Power curves for the Bonus Combi 300 kW and the optimized rotors for minimum noise and maximum production respectively.*

**Noise spectra**

Figure 5-4 shows the total predicted noise spectra for the different optimized rotors together with the Bonus Combi 300 kW, calculated for untripped flow.

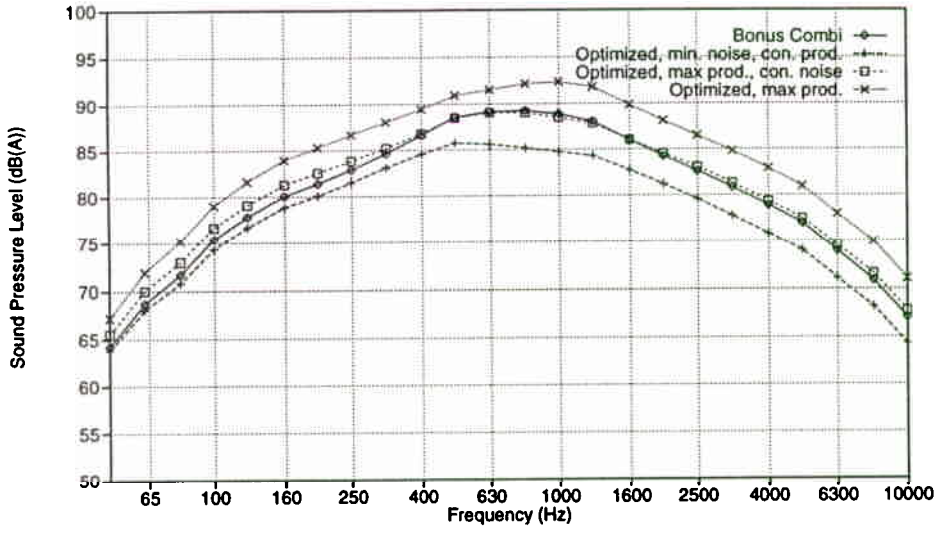


*Figure 5-4* *Total noise spectrum in dB(A) for the Bonus Combi 300 kW and the optimized rotors for minimum noise and maximum production, respectively.*

It can be seen, that the shape of the spectrum is common for the different rotors. The peak level frequency varies from 450 Hz to 1000 Hz. The peak level is however different. The rotor optimized for minimum noise is below the other rotors for all frequencies, and the optimized rotor for maximum production without noise concerns has the highest sound power levels, whereas the rotor optimized for maximum production with constraint on the noise has an almost equal spectrum as the Bonus Combi 300 kW.

The contributions from turbulent inflow is shown in Figure 5-5, and the contributions from airfoil self noise is shown in Figure 5-6.

The noise from turbulent inflow does not depend on the blade design. Since the rotor diameter is fixed, the dominating parameter is the tip speed and hence, the angular velocity. The difference on the turbulent inflow noise for the different rotors is therefore due to the change in angular velocity. The rotor optimized for minimum noise has the lowest power level, because of the lower tip speed. Since the noise from turbulent inflow is the dominating noise source, lower tip speed turns out to be the key parameter, when erecting wind turbines very close to residential areas.

The airfoil self noise does depend both on the blade design and on the tip speed. The explanation for the different shapes of the spectra for the different optimized rotors are therefore more difficult. It can be seen that the rotor, that is optimized for minimum noise has moved the peak frequency from around 550 Hz to 400 Hz. Higher frequencies are substantially reduced, whereas lower frequencies have remained almost unchanged. The noise sources with peak frequency at higher frequencies are tip noise and turbulent trailing edge noise, especially on the pressure side. These noise sources depend on the tip speed and on the airfoil free

stream, respectively. Since the airfoil relative velocity is reduced with the tip speed, this again turns out to be the key parameter.

The rotor optimized for maximum annual production with constraint on the noise, has an almost equal frequency spectrum as the Bonus Combi 300 kW. This could be expected, since the changes in the blade shape and tip speed are minor. Finally, the rotor optimized without noise concerns has higher power levels at higher frequencies, primarily from the increase in tip speed.

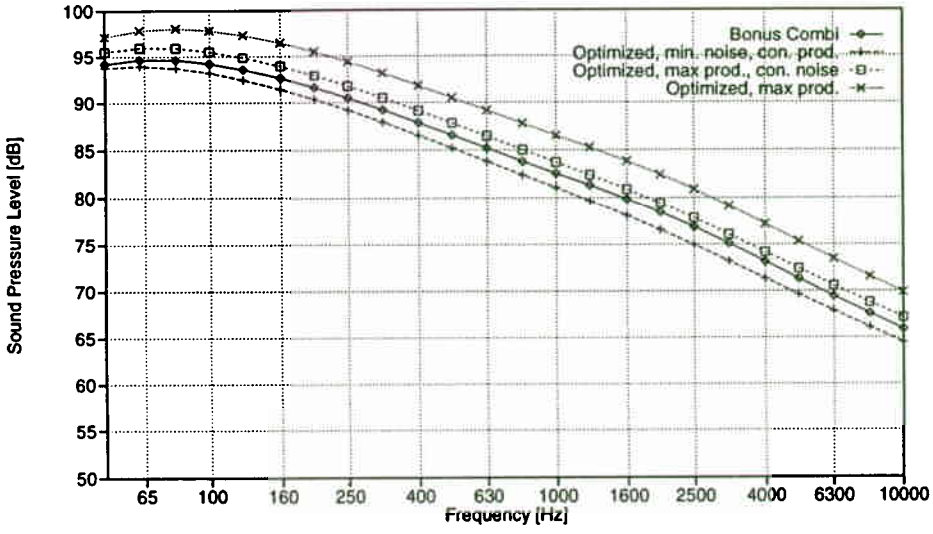


*Figure 5-5* *Turbulent inflow noise in dB for the Bonus Combi 300 kW and the optimized rotors for minimum noise and maximum production, respectively.*

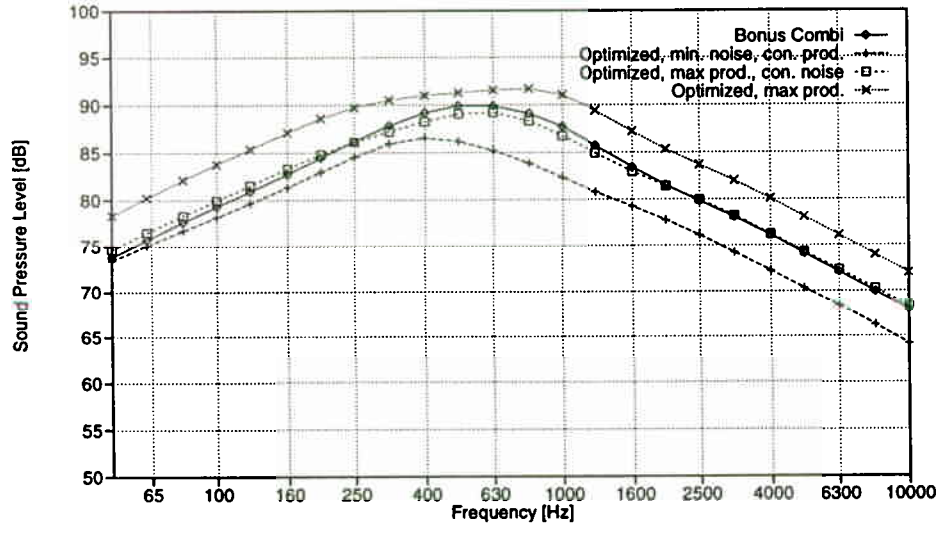


*Figure 5-6* *Airfoil self noise in dB for the Bonus Combi 300 kW and the optimized rotors for minimum noise and maximum production, respectively.*

## 5.3 Summary

In this chapter, three different optimization studies of the Bonus Combi 300 kW are carried out, using a design tool based on numerical optimization.

It is shown, that the total sound power level can be lowered around 3 dB(A), from 98.0 dB(A) to 94.9 dB(A), without lowering the annual production. This is done by decreasing the tip speed together with an increase in the blade solidity and fine adjustment of the tip pitch angle together with the twist distribution. The consequence of such an optimization is an increase in cost of the entire wind turbine, since both blade weight and extreme loads are increased. Even though the resulting rotor might not be suited for manufacturing, the optimization study has shown, that it is possible to include the noise emission as objective function in the optimization problem. Further work should incorporate the noise in the overall cost of the turbine for minimization of cost. Although it might be difficult, since the market value for a less noisier wind turbine is complex to determine.

The second case study shows, that the annual production can be increased by 2.0% without increasing the sound power level. This involves only minor changes in the blade design and hence, the cost. It seems therefore relevant to apply a constraint to the sound power level. Furthermore, it is easier to obtain sensible constraint values for the sound power level from codes and departmental orders, than to assign cost to the noise emission. Eventually, the overall cost of the wind turbine can be minimized subject to constraints on the total sound power level.

An optimization without noise concerns shows an increase in the annual production of 2.6%, but an additional increase in the sound power level of 3 dB(A). A constraint on the noise emission is therefore extremely important for the relevance of the optimization result.

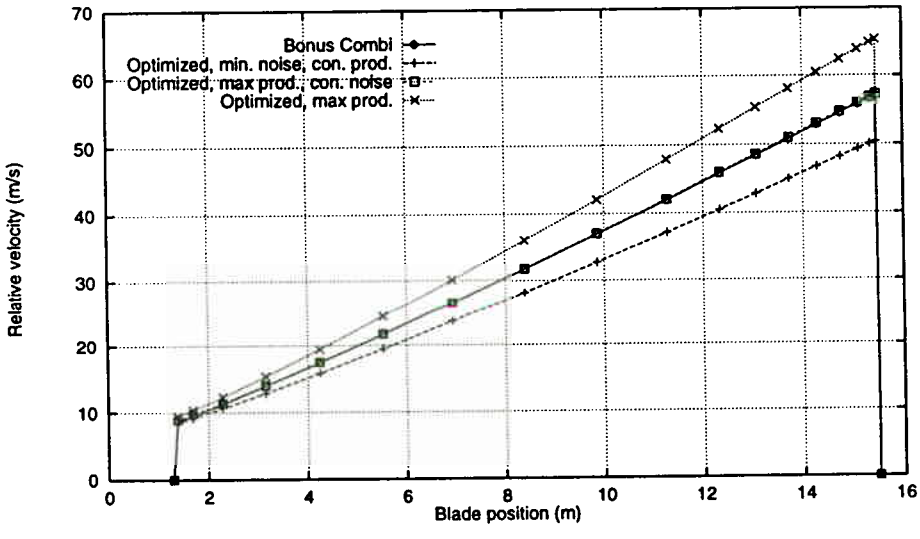


*Figure 5-7* *Relative velocity distribution at 8 m/s for the Bonus Combi 300 kW and the optimized rotors for minimum noise and maximum production, respectively.*

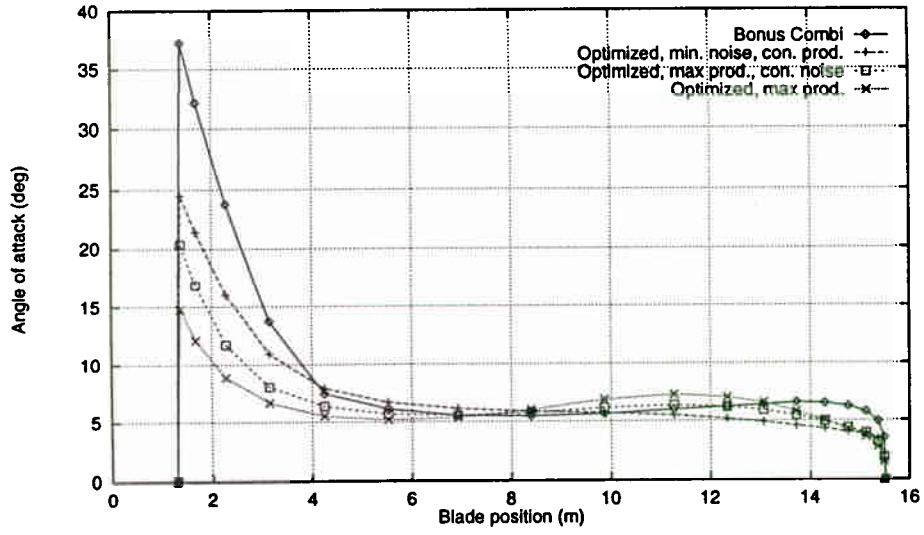


*Figure 5-8* *Angle of attack distribution at 8 m/s for the Bonus Combi 300 kW and the optimized rotors for minimum noise and maximum production respectively.*

The key parameter to noise reduction is the tip speed and hence, the airfoil free stream velocity along the blade. In Figure 5-7, this is calculated as a function of blade position for the different rotors at 8 m/s. The free stream velocity is lowered for the rotor optimized for minimum noise, whereas it is increased for the rotor optimized for maximum production.

Another important parameter is the local angle of attack. This is shown in Figure 5-8 for the different rotors at 8 m/s. All optimizations result in lower angles of attack at the root section and at the tip section. Because of the low free stream velocity, the root section is of minor importance. However, at the tip section, the rotor optimized for minimum noise has the lowest angles of attack, whereas the rotor optimized for maximum production without noise concerns has higher angles of attack. Apparently, the constraining/ minimization of the noise is capable of lowering the angles of attack at the entire tip section, and this is contributing to the overall reduction/ control of the noise.

The different optimization studies have shown, that noise can and should be taken into account by application of the noise prediction model together with present design tools.

# 6 Conclusion

In the present report, a semi-empirical noise prediction model for the aerodynamic noise from wind turbine rotors is implemented with aerodynamic calculations, and a design tool based on numerical optimization. The applied noise prediction model is semi-empirical and based on state of the art.

The model is divided into two main sources:

1. Turbulent inflow noise, originating from interaction between the rotor blade and the turbulence in the wind field, encountering the rotor. This is based on work by Lowson [5].

2. Airfoil self noise, from the interaction between the flow around the airfoil and the airfoil contour, radiated primarily from the airfoil trailing edge, based on Brooks, Pope & Marcolini [2]. The airfoil self noise can be further divided into a number of sources. Noise and boundary layer parameters have been measured in a wind tunnel environment and the noise measurements have been scaled with different geometry parameters from fundamental descriptions of the different noise sources.

The directivity from the airfoil leading and trailing edge is accounted for, so that the sound pressure level can be predicted for an observer at some position relative to the rotor. This is then transformed to the equivalent sound power level for a single source placed at the rotor center.

The spectra for the different noise sources are determined. Turbulent inflow noise is found to be the dominating noise source, especially at low frequencies. Airfoil self noise from laminar vortex shedding and blunt trailing edge vortex shedding are found difficult to include by using the present formulation. They are often not seen in measurements, and their nature has not yet been sufficiently incorporated into the model. The airfoil self noise sources from turbulence in the flow passing the trailing edge however have some importance at intermediate to high frequencies, whereas tip speed noise is found less important, though the peak frequency is high.

The prediction model is evaluated by comparing predictions with measurements and performing sensitivity studies on both important model parameters and rotor design parameters.

A number of model parameters are found important, and are further investigated: The difference between untripped and tripped flow, the trailing edge bluntness noise at different values of trailing edge thickness, the importance of the oncoming turbulence length scale and the distance from the rotor to the observer at the transformation from sound pressure level to sound power level.

Comparisons between predictions and measurements for the Vestas V27 and The Bonus Combi wind turbines show, that the sound power level is predicted with a deviation within 1.5 dB(A) from measurements. The spectrum shape is similar. Hence, there is a fair agreement in the absolute accuracy between predictions and measurements.

Comparisons at different wind speeds, tip pitch angles and tip speeds show, that, even though there is an offset on the absolute value of the sound power level, the relative behavior with the mentioned parameters is in very good agreement with

measurements. This is important because it opens for the possibility to perform reliable design studies and comparisons of noise emissions for different rotors in the design phase.

The directivity model, that is implemented is qualitatively investigated by calculating the radiation picture on the ground for the Vestas V27. This is compared with measurements, and good agreement is found. The noise level is maximum down- and upwind from the rotor, whereas it is lowered in the plane of rotation.

To further investigate the usability of the prediction model in the design phase, three different design studies are carried out, where it is tried to control the noise emission. The point of origin is the Bonus Combi. Focus is directed towards aerodynamic properties, whereas loads and cost are not calculated.

It is found, that the most important mechanism for noise reduction is to lower the tip speed, since this affects both airfoil self noise and the turbulent inflow noise. Another possibility is to decrease the angle of attack, especially at the tip region, where the emission from airfoil self noise is high.

An optimization of a rotor for minimum noise emission shows, that the total sound power level can be reduced by 3 dB(A) without loosing peak power and annual production. This however results in a rotor of higher cost because of increased extreme loads and heavier blades.

An optimization of a rotor for maximum production, but constraint on the noise not to exceed the level for Bonus Combi, shows a possible increase of 2.0% to the same sound power level. Fine adjustments to the blade design allows for this increase, which is believed not to change either cost or loads significantly. An additional optimization without noise concerns shows an increase in 3 dB(A) in the sound power level, gaining only 2.6% in the annual production.

The optimizations show, that noise concerns are extremely important in the design phase. One way to include noise is to evaluate cost for additional noise, so that this can be compared to the cost of the entire wind turbine. Another possibility is to constrain noise to values obtained from either customers requirements or departmental orders or codes. The latter can directly be done, if the absolute deviation on the sound power level is taken into account. It is difficult to estimate cost for noise emission, since this requires an analysis and understanding of the sales market situation. However, on the German market, the value of the produced energy is connected to the noise from the wind turbine producing the energy.

All in all, the implementation of the noise prediction model has been evaluated, and the model is found useful for absolute determination of the sound power level and especially at relative comparisons at parameter variations in the design phase for new less noisy rotors.

The present accuracy of the model should however not be over estimated. Several of the airfoil self noise sources are not yet modeled sufficiently accurate, and the turbulent inflow noise is based on a very simple approach. Hence, the degree of detail is in general too low, since the scaling parameters are few. A key point is the lack of sensitivity to the applied airfoils, since the airfoil self noise is being calculated only for the old NACA 0012 airfoil, that is no longer being used for wind turbines.

Instead of using measured boundary layer parameters for this airfoil for calibration, an airfoil prediction code should be used, so that the influence of different airfoils could affect the noise. This has been done by Lowson [6]. Another important issue is the need for additional measurements of different airfoils at operational conditions closer to wind turbines, so that the model can be better founded. In the future, it might even be possible to perform aeroacoustic calculations on different airfoils to determine their noise behavior, and directly implement these in the prediction model. However, though initial steps have been taken, this is not yet a possibility.

# References


[1] Hardin, J.C., Pope, D.S., 1994, "An acoustic/ Viscous Splitting Technique for Computational Aeroacoustics." J. Theoretical and Computational Fluid Dynamics, 6, pp 323-340.

[2] Brooks, T.F., Pope, D. S. and Marcolini, M.A., 1989, "Airfoil Self-Noise and Prediction.", NASA Reference Publication 1218, National Aeronautics and Space Administration, USA.

[3] Amiet, R.K., 1975, "Acoustic Radiation from an Airfoil in a Turbulent Stream." J. Sound Vibration, 41[4] pp. 407-420.

[4] Ffowcs Williams, J. E. and Hall, L.H., 1970, "Aerodynamic Sound Generation by Turbulent Flow in the vicinity of a Scattering Half-Plane." J. Fluid Mechanics 40, pp. 657-670.

[5] Lowson, M.V., 1993, "Assessment and Prediction of Wind Turbine Noise.", ETSU W/13/00284/REP.

[6] Lowson, M.V. and Fiddes, S.P., 1994, "Design Prediction Model for Wind Turbine Noise.", ETSU W/13/00317/REP.

[7] Fuglsang, P. and Madsen, H.A., 1995, "A Design Study of a 1 MW Stall Regulated Rotor.", Risø-R-799(EN), Risø National Laboratory, Denmark.

[8] Brooks, T.F. and Marcolini, M.A., 1986, "Airfoil Tip Vortex Formation Noise." AIAA Journal Vol 24[2], pp. 246 - 252.

[9] Grosveld, F.W., 1985, "Prediction of Broadband Noise from Horizontal Axis Wind Turbines.", J. Propulsion, 1[4], pp. 292-299.

[10] Dansk Ingeniørforening, 1992, "Dansk Ingeniørforenings og IngeniørSammenslutningens norm for last og sikkerhed for vindmøllekonstruktioner," (In Danish), DS 472, Teknisk Forlag, Denmark.

[11] "Bekendtgørelse om støj fra vindmøller" (In Danish), Miljøministeriets bekendtgørelse nr. 304 af 14. maj 1991.

[12] Committee Draft for an IEC standard, 1995, "Wind turbine generator systems -Part 10: Acoustic noise measurement techniques." Ref. 88/48/CDV.

[13] Jakobsen, J. and Andersen, B., 1993, "Aerodynamical Noise from Wind turbine Generators.", Danish Acoustical Institute. 1993-06-04, LI 464/93 D/70.89-464.1

[14] Jakobsen, J. and Andersen, B., 1995, "Aerodynamical Noise from Wind Turbines - Experiments with full scale rotors, change of pitch, trailing edges, and tip shapes.", Delta Acoustics & Vibration. AV 590/95.

[15] de Wolf, W.B., 1987, "Aerodynamisch geluid van windturbines." (In Dutch), NLR-MP87004U.

[16] Hubbard, H. H. and Shepherd, K. P., 1990, Wind turbine Acoustics.", NASA Technical Paper 3057 DOE/NASA/20320-77.

# A Wind turbine data

This appendix contains key parameters for the wind turbines used for comparison between predictions and measurements.

## Vestas V27 225 kW

| | |
|---|---|
| Rotor type | Upwind, pitch regulated |
| Rated power | 225 kW |
| Rotor diameter | 27 m |
| Hub height | 31.5 m |
| Number of blades | 3 |
| Maximum chord | 1.33 m |
| Tip chord | 0.47 m |
| Maximum twist | 14.0° |
| Airfoils | Modified NACA 63200 series |
| Angular velocity | 43.0 rpm |
| Tip pitch angle | Various between -1.5° and 3.5° |

## Bonus Combi 300 kW

| | |
|---|---|
| Rotor type | Upwind, stall regulated |
| Rated power | 300 kW |
| Rotor diameter | 31 m |
| Hub height | 30.7 m |
| Number of blades | 3 |
| Maximum chord | 1.58 m |
| Tip chord | 0.50 m |
| Maximum twist | 16.0° |
| Airfoils | NACA 63400/ NACA 63200 series |
| Angular velocity | 35.0 rpm |
| Tip pitch angle | -1.8° |

**Bibliographic Data Sheet** **Risø-R-867(EN)**

Title and author(s)

# Implementation and Verification of an Aeroacoustic Noise Prediction Model for Wind Turbines

Peter Fuglsang, Helge Aagaard Madsen

ISBN
87-550-2149-2

ISSN
0106-2840

Dept. or group
Test Station for Wind Turbines
Dept. of Meteorology and Wind Energy

Date
March 1996

Groups own reg. number(s)

Project/contract No.
ENS 1364/93-0006
ENS 1364/93-0001

| Pages | Tables | Illustrations | References |
|---|---|---|---|
| 53 | 1 | 31 | 17 |

Abstract (Max. 2000 char)

The present report concerns a semi-empirical noise prediction model for the aerodynamic noise from wind turbine rotors. It covers both turbulent inflow noise and airfoil self noise. The noise prediction model cooperates with aerodynamic calculations and a design tool based on numerical optimization.

The spectra for different noise sources are determined and the total noise is compared to measurements. Fair agreement is obtained for the sound power level, with deviations within 1.5 dB(A) on the absolute value. The shape of the predicted spectrum fits well to measurements. A sensitivity study on different design parameters is performed. Measurements agree well with predictions for variations of the wind speed, tip pitch angle and tip speed. This is encouraging, since a reliable relative comparison between different rotors seems possible.

By use of a numerical optimization tool for wind turbines, several optimization studies are carried out, with the starting point at an existing 300 kW rotor. Optimizing for minimum noise is possible and this lowers the sound power level by 3 dB(A), a substantial reduction. The resulting rotor has however increased cost and extreme loads. Therefore cost should also be estimated for the noise emission. It is possible to control the resulting sound power level by optimizing for maximum production or minimum cost with constraints on the noise. This allows for inclusion of noise limits from customers or codes of practice directly in the design process. An optimization without noise concerns emphasizes the importance of this, since this increases the noise by 3 dB(A), without a significant improvement in the annual production.

The prediction model is useful for parameter investigations and design studies for a new generation of less noisy wind turbines having low cost. However, the degree of detail for the boundary layer parameters should be increased by application of an airfoil prediction code. Finally, verification should be extended with measurements from rotors with different airfoils.

Descriptors INIS/EDB
ACOUSTIC MEASUREMENTS; AERODYNAMICS; FORECASTING; MATHEMATICAL MODELS; NOISE; OPTIMIZATION; ROTORS; VERIFICATION; WIND TURBINES

Available on request from:
Information Service Department, Risø National Laboratory (Afdelingen for Informationsservice, Forskningscenter Risø)
P.O. Box 49, DK-4000 Roskilde, Denmark
Phone (+45) 46 77 46 77, ext. 4004/4005 • Telex 43 116 • Fax (+45) 46 75 56 27

RISØ

## Objective

Risø's objective is to provide society and industry with new opportunities for development in three main areas:

- *Energy technology and energy planning*
- *Environmental aspects of energy, industrial and agricultural production*
- *Materials and measuring techniques for industry*

In addition, Risø advises the authorities on nuclear issues.

## Research profile

Risø's research is strategic, which means that it is long-term and directed toward areas which technological solutions are called for, whether in Denmark or globally. The reasearch takes place within 11 programme areas:

- *Wind energy*
- *Energy materials and energy technologies for the future*
- *Energy planning*
- *Environmental impact of atmospheric processes*
- *Processes and cycling of matter in ecosystems*
- *Industrial safety*
- *Environmental aspects of agricultural production*
- *Nuclear safety and radiation protection*
- *Structural materials*
- *Materials with special physical and chemical properties*
- *Optical measurement techniques and information processing*

## Transfer of Knowledge

Risø's research results are transferred to industry and authorities through:

- *Co-operation on research*
- *Co-operation in R&D consortia*
- *R&D clubs and exchange of researchers*
- *Centre for Advanced Technology*
- *Patenting and licencing activities*

And to the world of science through:

- *Publication activities*
- *Network co-operation*
- *PhD education and post docs*

## Key Figures

Risø has a staff of more than 900, including more than 300 researchers and 100 PhD students and post docs. Risø's 1996 budget totals DKK 471 m, of which 45 % come from research programmes and commercial contracts, while the remainder is covered by government appropriations.

**Risø-R-867(EN)**
**ISBN 87-550-2149-2**
**ISSN 0106-2840**

Available on request from:
**Information Service Department**
**Risø National Laboratory**
P.O. Box 49, DK-4000 Roskilde, Denmark
Phone +45 46 77 46 77, ext. 4004/4005
Telex 43116, Fax +45 46 75 56 27
http://www.risoe.dk
e-mail: risoe@risoe.dk